# Exact Potts Model Partition Functions for Strips of the Square Lattice

Shu-Chiuan Chang[(a)*] Jesús Salas[(b)†] Robert Shrock[(a)**]

(a) C. N. Yang Institute for Theoretical Physics
State University of New York
Stony Brook, N. Y. 11794-3840
USA

(b) Departamento de Física Teórica
Facultad de Ciencias
Universidad de Zaragoza
Zaragoza 50009
Spain

**Abstract**

We present exact calculations of the Potts model partition function $Z(G,q,v)$ for arbitrary $q$ and temperature-like variable $v$ on $n$-vertex square-lattice strip graphs $G$ for a variety of transverse widths $L_t$ and for arbitrarily great length $L_\ell$, with free longitudinal boundary conditions and free and periodic transverse boundary conditions. These have the form $Z(G,q,v) = \sum_{j=1}^{N_{Z,G,\lambda}} c_{Z,G,j}(\lambda_{Z,G,j})^{L_\ell}$. We give general formulas for $N_{Z,G,j}$ and its specialization to $v=-1$ for arbitrary $L_t$ for both types of boundary conditions, as well as other general structural results on $Z$. The free energy is calculated exactly for the infinite-length limit of the graphs, and the thermodynamics is discussed. It is shown how the internal energy calculated for the case of cylindrical boundary conditions is connected with critical quantities for the Potts model on the infinite square lattice. Considering the full generalization to arbitrary complex $q$ and $v$, we determine the singular locus $\mathcal{B}$, arising as the accumulation set of partition function zeros as $L_\ell \to \infty$, in the $q$ plane for fixed $v$ and in the $v$ plane for fixed $q$.

*email: shu-chiuan.chang@sunysb.edu
†email: salas@laurel.unizar.es
**email: robert.shrock@sunysb.edu

# 1 Introduction

The $q$-state Potts model has served as a valuable model for the study of phase transitions and critical phenomena [1]-[3]. On a lattice, or, more generally, on a (connected) graph $G$, at temperature $T$, this model is defined by the partition function

$$Z(G,q,v) = \sum_{\{\sigma_n\}} e^{-\beta\mathcal{H}} \tag{1.1}$$

with the (zero-field) Hamiltonian

$$\mathcal{H} = -J \sum_{\langle ij \rangle} \delta_{\sigma_i \sigma_j} \tag{1.2}$$

where $\sigma_i = 1, ..., q$ are the spin variables on each vertex $i \in G$; $\beta = (k_B T)^{-1}$; and $\langle ij \rangle$ denotes pairs of adjacent vertices. The graph $G = G(V, E)$ is defined by its vertex set $V$ and its edge set $E$; we denote the number of vertices of $G$ as $n = n(G) = |V|$ and the number of edges of $G$ as $e(G) = |E|$. We use the notation

$$K = \beta J \ , \quad a = e^K = u^{-1} \ , \quad v = a - 1 \tag{1.3}$$

so that the physical ranges are (i) $v \geq 0$ corresponding to $\infty \geq T \geq 0$ for the Potts ferromagnet, and (ii) $-1 \leq v \leq 0$, corresponding to $0 \leq T \leq \infty$ for the Potts antiferromagnet. One defines the (reduced) free energy per site $f = -\beta F$, where $F$ is the actual free energy, via

$$f(G,q,v) = n^{-1} \ln[Z(G,q,v)] \tag{1.4}$$

and, in the $n \to \infty$ limit,

$$f(\{G\},q,v) = \lim_{n\to\infty} n^{-1} \ln[Z(G,q,v)] \tag{1.5}$$

where we use the symbol $\{G\}$ to denote $\lim_{n\to\infty} G$ for a given family of graphs.

Let $G' = (V, E')$ be a spanning subgraph of $G$, i.e. a subgraph having the same vertex set $V$ and an edge set $E' \subseteq E$. Then $Z(G,q,v)$ can be written as the sum [4]

$$Z(G,q,v) = \sum_{G' \subseteq G} q^{k(G')} v^{e(G')} \tag{1.6}$$

where $k(G')$ and $e(G')$ denote respectively the number of connected components and the number of edges of $G'$. Since we only consider connected graphs $G$, we have $k(G) = 1$. The formula (1.6) enables one to generalize $q$ from $\mathbb{Z}_+$ to $\mathbb{R}_+$ and, indeed, to $\mathbb{C}$. The Potts model

partition function on a graph $G$ is essentially equivalent to the Tutte polynomial [5]-[7] and Whitney rank polynomial [2], [8]-[10] for this graph.

In this paper we shall present exact calculations of the Potts model partition function $Z(G,q,v)$, for arbitrary $q$ and $v$, on square-lattice strip graphs $G$ of various widths $L_t$ and arbitrarily great length $L_\ell$, with boundary conditions that are (i) free in both longitudinal and transverse directions, denoted "open" and (ii) periodic in the transverse direction and free in the longitudinal direction, denoted "cylindrical". Specifically, we shall consider strips with $L_t$ vertices along a transverse slice (hence $L_t$ edges on this slice in the case of cylindrical boundary conditions and $L_t-1$ edges in the case of free boundary conditions) and $L_\ell$ vertices along a longitudinal slice. We shall often denote the strip with open boundary conditions as $(L_t)_{\rm F} \times (L_\ell)_{\rm F}$ and the strip with cylindrical boundary conditions as $(L_t)_{\rm P} \times (L_\ell)_{\rm F}$. Previous related calculations of $Z(G,q,v)$ for arbitrary $q$ and $v$ on fixed-width, arbitrary-length lattice strip graphs are in [11]-[13] for the square lattice, in [14] for the triangular lattice, in [15] for the honeycomb lattice, and in [16] for the square lattice with next-nearest-neighbor edges (bonds). Some general properties are given in [17, 18]. Calculations of $Z(G,q,v)$ for arbitrary $q$ and $v$ on finite sections of lattices have been given in [19, 20] and used for studies of zeros in the $q$ and $v$ plane (the latter being complex-temperature or Fisher zeros [21]); for fixed positive integral values of $q$, such calculations have been given, e.g., in [22]-[28]. Since the Ising case $q = 2$ is exactly solvable on two-dimensional lattices, one can calculate exactly the complex-temperature phase boundaries that are the accumulation sets of the complex-temperature zeros in the thermodynamic limit (e.g., [29]-[41] and references therein).

There are several motivations for the present work. Clearly, new exact calculations of Potts model partition functions are of value in their own right. Since the results apply for arbitrary length, one can take the limit of infinite length and calculate the free energy and specific heat for the Potts model with any $q$ and various widths. In addition, it was shown [12] that these calculations can give insight into the complex-temperature phase diagram of the 2D Potts model on the given lattice. This is useful since the 2D Potts model has never been solved except in the (zero-field) $q = 2$ Ising case.

Various special cases of the Potts model partition function are of interest. One special case is the zero-temperature limit of the Potts antiferromagnet (AF), i.e., $v = -1$. For sufficiently large $q$, on a given lattice or graph $G$, this exhibits nonzero ground state entropy (without frustration). Such nonzero ground state entropy is an exception to the third law of thermodynamics [42, 43]. It is equivalent to a ground state degeneracy per site (vertex), $W > 1$, since $S_0 = k_B \ln W$. The $T = 0$ (i.e., $v = -1$) partition function of the above-

mentioned $q$-state Potts antiferromagnet (PAF) on $G$ satisfies

$$Z(G,q,-1) = P(G,q) \tag{1.7}$$

where $P(G,q)$ is the chromatic polynomial (in $q$) expressing the number of ways of coloring the vertices of the graph $G$ with $q$ colors such that no two adjacent vertices have the same color [8, 44, 45]. The minimum number of colors necessary for this coloring is the chromatic number of $G$, denoted $\chi(G)$. We have

$$W(\{G\},q) = \lim_{n\to\infty} P(G,q)^{1/n} \ . \tag{1.8}$$

Some previous related works on chromatic polynomials and the $W$ function are [46]-[77]. Using the formula (1.6) for $Z(G,q,v)$, one can generalize $q$ from $\mathbb{Z}_+$ not just to $\mathbb{R}_+$ but to $\mathbb{C}$ and $a$ from its physical ferromagnetic and antiferromagnetic ranges $0 \le v \le \infty$ and $-1 \le v \le 0$ to $v \in \mathbb{C}$. A subset of the zeros of $Z$ in the two-complex dimensional space $\mathbb{C}^2$ defined by the pair of variables $(q,v)$ can form an accumulation set in the $n \to \infty$ limit, denoted $\mathcal{B}$, which is the continuous locus of points where the free energy is nonanalytic. This locus is determined as the solution to a certain $\{G\}$-dependent equation [11, 12]. For a given value of $v$, one can consider this locus in the $q$ plane, and we denote it as $\mathcal{B}_q(\{G\},v)$. In the special case $v=-1$ where the partition function is equal to the chromatic polynomial, the zeros in $q$ are the chromatic zeros, and $\mathcal{B}_q(\{G\},v=-1)$ is their continuous accumulation set in the $n \to \infty$ limit. Previous works have given exact calculations of the chromatic polynomials and nonanalytic loci $\mathcal{B}_q$ for various families of graphs. With the exact Potts partition function, one can study $\mathcal{B}_q$ for arbitrary temperature in both the antiferromagnetic and ferromagnetic cases and, for a given value of $q$, one can study the continuous accumulation set of the zeros of $Z(G,q,v)$ in the $v$ plane; this will be denoted $\mathcal{B}_v(\{G\},q)$. (Where the context is clear, we shall refer to these accumulation sets in the $q$ and $v$ plane as just $\mathcal{B}$.)

Following the notation in [56] and our other earlier works on $\mathcal{B}_q(\{G\})$ for $v=-1$, we denote the maximal region in the complex $q$ plane to which one can analytically continue the function $W(\{G\},q)$ from physical values where there is nonzero ground state entropy as $R_1$. The maximal value of $q$ where $\mathcal{B}_q$ intersects the (positive) real axis was labelled $q_c(\{G\})$. Thus, region $R_1$ includes the positive real axis for $q > q_c(\{G\})$. Correspondingly, in the studies of complex-temperature phase diagrams of spin models [35, 36] a nomenclature was used according to which the complex-temperature extension(CTE) of the physical paramagnetic phase was denoted as (CTE)PM, which will simply be labelled PM here, the extension being understood, and similarly with ferromagnetic (FM) and antiferromagnetic (AFM) phases; other complex-temperature phases, having no overlap with any physical phase, were denoted

$O_j$ (for "other"), with $j$ indexing the particular phase. Here we shall continue to use this notation for the respective slices of $\mathcal{B}$ in the $q$ and $v$ planes.

We record some special values of $Z(G,q,v)$ below, beginning with the $q=0$ special case

$$Z(G,0,v) = 0 \tag{1.9}$$

which implies that $Z(G,q,v)$ has an overall factor of $q$, as is also clear from (1.6). In general (and for all the graphs considered here), this is the only overall factor that it has. We also have

$$Z(G,1,v) = \sum_{G' \subseteq G} v^{e(G')} = a^{e(G)} \ . \tag{1.10}$$

For temperature $T=\infty$, i.e., $v=0$,

$$Z(G,q,0) = q^{n(G)} \ . \tag{1.11}$$

where $n(G)$ is the total number of sites of $G$. Further,

$$Z(G,q,-1) = P(G,q) = \Big[ \prod_{s=0}^{\chi(G)-1} (q-s) \Big] U(G,q) \tag{1.12}$$

where $U(G,q)$ is a polynomial in $q$ of degree $n(G)-\chi(G)$.

Another basic property, evident from eq. (1.6), is that (i) the zeros of $Z(G,q,v)$ in $q$ for real $v$ and hence also the continuous accumulation set $\mathcal{B}_q$ are invariant under the complex conjugation $q \to q^*$; (ii) the zeros of $Z(G,q,v)$ in $v$ or equivalently $a$ for real $q$ and hence also the continuous accumulation set $\mathcal{B}_v$ are invariant under the complex conjugation $v \to v^*$. In certain cases one must take account of the noncommutativity [56, 12]

$$\lim_{n\to\infty} \lim_{q\to q_s} Z(G,q,v)^{1/n} \ne \lim_{q\to q_s} \lim_{n\to\infty} Z(G,q,v)^{1/n} \ . \tag{1.13}$$

A general form for the Potts model partition function for the strip graphs considered here, or more generally, for recursively defined families of graphs comprised of $m$ repeated subunits (e.g. the columns of squares of transverse width $L_t$ vertices that are repeated $L_\ell$ times in the longitudinal direction to form an $L_\ell \times L_t$ strip of a regular lattice with some specified boundary conditions), is [12]

$$Z(G,q,v) = \sum_{j=1}^{N_{Z,G,\lambda}} c_{G,j} (\lambda_{G,j})^m \tag{1.14}$$

where the coefficients $c_{G,j}$ and corresponding terms $\lambda_{G,j}$, as well as the total number $N_{Z,G,\lambda}$ of these terms, depend on the type of recursive graph $G$ (width and boundary conditions)

but not its length. In the special case $v = -1$ where $Z$ reduces to the chromatic polynomial (zero-temperature Potts antiferromagnet), eq. (1.14) reduces to the form [52]

$$P(G,q) = \sum_{j=1}^{N_{P,G,\lambda}} c_{G,j} (\lambda_{P,G,j})^m \ . \tag{1.15}$$

For the lattice strips of interest here, we define the following explicit notation. Let $N_{Z,sq,BC_t \ BC_\ell,L_t,\lambda}$ denote the total number of $\lambda$'s for the square-lattice strip with the transverse ($t$) and longitudinal ($\ell$) boundary conditions $BC_t$ and $BC_\ell$ of width $L_t$. Henceforth where no confusion will result, we shall suppress the $\lambda$ subscript. The explicit labels are $N_{Z,sq,FF,L_t}$ and $N_{Z,tri,FF,L_t}$ for the strips of the square and triangular lattices with free boundary conditions, and $N_{Z,sq,PF,L_t}$ and $N_{Z,tri,PF,L_t}$ for the strips of these respective lattices with cylindrical boundary conditions. In the special case $v = -1$, our nomenclature for the corresponding total numbers of $\lambda$'s in the chromatic polynomials are listed below, together with the labels used for these numbers in [17]:

$$N_{P,sq,FF,L_t} \equiv \mathrm{SqFree}(L_t) \tag{1.16}$$

$$N_{P,tri,FF,L_t} \equiv \mathrm{TriFree}(L_t) \tag{1.17}$$

$$N_{P,sq,PF,L_t} \equiv \mathrm{SqCyl}(L_t) \tag{1.18}$$

$$N_{P,tri,PF,L_t} \equiv \mathrm{TriCyl}(L_t) \ . \tag{1.19}$$

The Potts ferromagnet has a zero-temperature phase transition in the $L_\ell \to \infty$ limit of the strip graphs considered here. However, in contrast to the infinite-length, finite-width lattice strips with periodic (or twisted periodic) longitudinal boundary conditions, where this property was reflected in the feature that $\mathcal{B}$ in the $u = 1/a$ plane passes through the $T = 0$ point $u = 0$ and hence is noncompact in the $a$ plane, for infinite-length strips with free longitudinal boundary conditions, $\mathcal{B}$ is generically compact in the $a$ (equivalently, the $v$) plane.

# 2 General Structural Properties

In this section we give some results for the numbers of $\lambda$'s that enter in the respective chromatic polynomials and Potts model partition functions for the strips of interest here. Recall the definitions of the Catalan number $C_n$ and Motzkin number $M_n$ [78]-[81]:

$$C_n = \frac{1}{n+1}\binom{2n}{n} \tag{2.1}$$

$$M_n = \sum_{j=0}^{n} (-1)^j C_{n+1-j} \binom{n}{j} \tag{2.2}$$

These numbers occur in many combinatoric applications [78]-[83]. Among these is the construction of non-intersecting chords on a circle; the number of ways of connecting a subset of $n$ points on a circle by non-intersecting chords is $M_n$, while the number of ways of completely connecting $2n$ points on the circle by non-intersecting chords is $C_n$. Summing over subsets of points connected by chords, this yields the known relation

$$M_n = \sum_{k=0}^{[\frac{n}{2}]} \binom{n}{2k} C_k \ . \tag{2.3}$$

where $[\nu]$ denotes the integral part of $\nu$. These numbers have the asymptotic behaviors

$$C_n \sim \pi^{-1/2} n^{-3/2} 4^n \Big[1 + O(n^{-1})\Big] \quad \text{as} \quad \text{n} \to \infty \tag{2.4}$$

$$M_n \sim 3^{3/2} 2^{-1} \pi^{-1/2} n^{-3/2} 3^n \Big[1 + O(n^{-1})\Big] \quad \text{as} \quad \text{n} \to \infty \ . \tag{2.5}$$

Ref. [18] derived expressions for the total number of $\lambda$'s in $Z$ and $P$ with periodic boundary conditions in the longitudinal direction and free boundary conditions in the transverse direction. We denote such quantities respectively as $N_{Z,sqtri,FP,L_t}$ and $N_{P,sqtri,FP,L_t}$, where *sqtri* means either square or triangular:

$$N_{Z,sqtri,FP,L_t} = \binom{2L_t}{L_t} \tag{2.6}$$

$$N_{P,sqtri,FP,L_t} = 2(L_t - 1)! \sum_{j=0}^{[\frac{L_t}{2}]} \frac{(L_t - j)}{(j!)^2 (L_t - 2j)!} \ . \tag{2.7}$$

These have the leading asymptotic behaviors $N_{Z,sqtri,FP,L_t} \sim L_t^{-1/2}\ 4^{L_t}$ and $N_{P,sqtri,FP,L_t} \sim L_t^{-1/2}\ 3^{L_t}$ as $L_t \to \infty$.

## 2.1 $N_{P,G,BC,L_t}$

Recall that for the open strip of the triangular lattice of width $L_t$, Ref. [17] obtained the result

$$N_{P,tri,FF,L_t} = M_{L_t - 1} \ . \tag{2.1.1}$$

The proof of this was based on the property that there is a one-one correspondence between the number of distinct eigenvalues $\lambda$ of the transfer matrix and the number of non-crossing, non-nearest-neighbor partitions of the set $\{1, 2, ..., L_t\}$. But the latter number is precisely the Motzkin number $M_{L_t - 1}$.

Table 1: Numbers of $\lambda$'s for the chromatic polynomial for the strips of the triangular and square lattices having free and cylindrical boundary conditions and various widths $L_t$.

| $L_t$ | $N_{P,tri,FF,L_t}$ | $N_{P,sq,FF,L_t}$ | $2N_{P,sq,FF,L_t}$ $-N_{P,tri,FF,L_t}$ | $d_{L_t}$ | $N_{P,tri,PF,L_t}$ | $N_{P,sq,PF,L_t}$ | $2N_{P,sq,PF,L_t}$ $-N_{P,tri,PF,L_t}$ | $L_t N_{P,tri,PF,L_t}$ $-d_{L_t}$ |
|---|---|---|---|---|---|---|---|---|
| 1 | 1 | 1 | 1 | 1 | 1 | 1 | 1 | 0 |
| 2 | 1 | 1 | 1 | 1 | 1 | 1 | 1 | 1 |
| 3 | 2 | 2 | 2 | 1 | 1 | 1 | 1 | 2 |
| 4 | 4 | 3 | 2 | 3 | 2 | 2 | 2 | 5 |
| 5 | 9 | 7 | 5 | 6 | 2 | 2 | 2 | 4 |
| 6 | 21 | 13 | 5 | 15 | 5 | 5 | 5 | 15 |
| 7 | 51 | 32 | 13 | 36 | 6 | 6 | 6 | 6 |
| 8 | 127 | 70 | 13 | 91 | 15 | 14 | 13 | 29 |
| 9 | 323 | 179 | 35 | 232 | 28 | 22 | 16 | 20 |
| 10 | 835 | 435 | 35 | 603 | 67 | 51 | 35 | 67 |
| 11 | 2188 | 1142 | 96 | 1585 | 145 | 95 | 45 | 10 |
| 12 | 5798 | 2947 | 96 | 4213 | 368 | 232 | 96 | 203 |
| 13 | 15511 | 7889 | 267 | 11298 | 870 | 498 | 126 | 12 |
| 14 | 41835 | 21051 | 267 | 30537 | 2211 | 1239 | 267 | 417 |

Now the number of $\lambda$'s for the open square-lattice strip with a given width $L_t$ is less than for the open triangular strip of this width because some of the symmetry under reflection about the longitudinal axis, which renders some of the partitions equivalent to each other. We proceed to derive this number. Because of this reflection symmetry, $2N_{P,sq,FF,L_t} - N_{P,tri,FF,L_t}$ gives the number of non-crossing non-nearest-neighbor partitions for a transverse slice that is symmetric under this reflection.

Using this observation, we proceed to derive the following result:

**Theorem 1**

$$2N_{P,sq,FF,L_t} - N_{P,tri,FF,L_t} = \frac{1}{2} N_{P,sqtri,FP,[\frac{L_t+1}{2}]} \ . \tag{2.1.2}$$

*Proof.* Let us denote $2N_{P,sq,FF,L_t} - N_{P,tri,FF,L_t}$ by $X_{L_t}$ for short. To show the general method of the proof, we first list, for small $L_t$, the sets $\mathbf{P}_{X_{L_t}}$ of partitions having the above-mentioned reflection symmetry: $\mathbf{P}_{X_1} = \{1\}$, $\mathbf{P}_{X_2} = \{1\}$, $\mathbf{P}_{X_3} = \{1, \delta_{1,3}\}$, $\mathbf{P}_{X_4} = \{1, \delta_{1,4}\}$, $\mathbf{P}_{X_5} = \{1, \delta_{2,4}, \delta_{1,5}, \delta_{2,4}\delta_{1,5}, \delta_{1,3,5}\}$, $\mathbf{P}_{X_6} = \{1, \delta_{2,5}, \delta_{1,6}, \delta_{2,5}\delta_{1,6}, \delta_{1,3}\delta_{4,6}\}$. Here it can be seen that going from the partition for an odd width $L_t$ to the partition for the next greater width, $L_t + 1$, one only has to split the central vertex into two vertices (one connected only to vertices left of center, the other only to vertices right of center) without otherwise changing the partitions. Hence,

$$X_{L_t+1} = X_{L_t} \quad \text{for odd } L_t \ . \tag{2.1.3}$$

Going from the partition for an even width $L_t$ to the partition for the next greater $L_t + 1$, there are two possibilities. The first possibility is that there is no delta function connecting any vertex in the set $\{1, 2, .., L_t/2\}$ and the corresponding vertex in the set $\{L_t/2+1, L_t/2+2, .., L_t\}$. Let us denote the number of these kinds of partitions by $X_{L_t,a}$, which is equal to $N_{P,tri,FF,L_t/2}$. In this case, one can add a vertex in the middle. The second possibility is that there is more than one delta function connecting the two vertex sets mentioned above. Let

us denote the number of these kinds of partitions by $X_{L_t,b}$. Clearly, $X_{L_t,a} + X_{L_t,b} = X_{L_t}$ for the case of even $L_t$ considered here. In this case, one can either add a vertex in the middle without any further delta function or have one more delta function connecting this middle vertex and the nearest vertex pair which are already connected by a delta function.

Another way to get a partition for $L_t + 1$ vertices is to start with a basis consisting of $L_t - 1$ vertices. Here one splits the central vertex for $L_t - 1$ into three vertices with the upper and lower vertices connected by a delta function. The number of these types of partition is $X_{L_t-1}$. With eqs. (2.1.1) and (2.1.3), we obtain

$$\begin{aligned} X_{L_t+1} &= X_{L_t,a} + 2X_{L_t,b} + X_{L_t-1} && (2.1.4)\\ &= M_{\frac{L_t}{2}-1} + 2(X_{L_t-1} - M_{\frac{L_t}{2}-1}) + X_{L_t-1} && (2.1.5)\\ &= 3X_{L_t-1} - M_{\frac{L_t}{2}-1} \quad \text{for even } L_t\ . && (2.1.6) \end{aligned}$$

Setting $L_t = 2\ell$ in eq. (2.1.6), we have

$$X_{2\ell+1} = 3^\ell - 3^{\ell-1}M_0 - 3^{\ell-2}M_1 - ... - M_{\ell-1} = X_{2\ell+2}\ . \tag{2.1.7}$$

We observe from eq. (2.1.6) that $2X_{2\ell+1}$ has the same recursion relation and initial values as $N_{P,L_t+1,\lambda}$ in eq. (5.1) in [18], which proves eq. (2.1.2). □

We remark that this proof evidently links together results for two different sets of longitudinal boundary conditions.

**Theorem 2**

$$N_{P,sq,FF,L_t} = \frac{1}{2}M_{L_t-1} + \frac{1}{2}(L'_t - 1)!\sum_{j=0}^{[\frac{L'_t}{2}]} \frac{(L'_t - j)}{(j!)^2(L'_t - 2j)!} \tag{2.1.8}$$

where

$$L'_t = \left[\frac{L_t + 1}{2}\right]\ . \tag{2.1.9}$$

*Proof* This follows from Theorem 1 and the expressions for $N_{P,tri,FF,L_t}$ and $N_{P,sqtri,FP,[(L_t+1)/2]}$. □.

**Corollary 1**. $N_{P,sq,FF,L_t}$ has the asymptotic behavior

$$N_{P,sq,FF,L_t} \sim 3^{1/2}2^{-2}\pi^{-1/2}L_t^{-3/2}3^{L_t}\Big[1 + O(L_t^{-1})\Big] \quad \text{as} \quad L_t \to \infty\ . \tag{2.1.10}$$

*Proof.* This follows directly from the asymptotic behaviors given above for the Motzkin number and for $N_{P,sqtri,FP,L_t}$, which show that as $L_t \to \infty$, the third term, $N_{P,sqtri,FP,[(L_t+1)/2]}$, is negligibly small compared with the first two in eq. (2.1.2). The latter, in turn, is a consequence of the fact that the leading exponential asymptotic behavior, as $L_t \to \infty$, of the dominant terms is $\sim 3^{L_t}$ while that of the third term is $\sim 3^{L_t/2}$.

**Corollary 2**.

$$\lim_{N_t\to\infty} \frac{N_{P,sq,FF,N_t}}{N_{P,tri,FF,N_t}} = \frac{1}{2} \ . \tag{2.1.11}$$

*Proof.* This follows from (2.1.2) and the asymptotic behaviors given above.

In [17] it was conjectured that $\lim_{L_t\to\infty} \mathrm{SqFree}(L_t)/\mathrm{TriFree}(L_t) = 1/2$. Our theorem and corollary 2 prove this conjecture.

We next consider the strips with cylindrical boundary conditions and the quantity $2N_{P,sq,PF,L_t} - N_{P,tri,PF,L_t}$. We find that the following relation holds for $1 \le L_t \le 14$ and conjecture that it holds for all widths $L_t$:

**Conjecture 1** For arbitrary $L_t$,

$$2N_{P,sq,PF,L_t} - N_{P,tri,PF,L_t} = \begin{cases} \frac{1}{2} N_{P,sqtri,FP,\frac{L_t}{2}} & \text{for even } L_t \\ \frac{1}{4} N_{P,sqtri,FP,\frac{L_t+1}{2}} - \frac{1}{2} R_{\frac{L_t-1}{2}} & \text{for odd } L_t \ge 3 \end{cases} \tag{2.1.12}$$

where $R_n$ is the Riordan number, which may be defined via the generating function [81],[84]

$$\frac{1 + x - (1 - 2x - 3x^2)^{1/2}}{2x(1+x)} = \sum_{n=0}^{\infty} R_n x^n \tag{2.1.13}$$

or, for $n \ge 2$, by [85]

$$R_n = (-1)^n \sum_{j=1}^{n-1} (-1)^{j+1} M_j \quad \text{for } n \ge 2 \ . \tag{2.1.14}$$

Note that $R_{L_t}$ is equal to the quantity $d_{L_t}$ given in Table 1 for $L_t \ge 2$.

**Theorem 3**.

$$N_{P,tri,PF,L_t} = \frac{d_{L_t} + L_t - 1}{L_t} \quad \text{for prime } L_t \ . \tag{2.1.15}$$

*Proof* As shown in [17], $d_{L_t}$ is the number of non-crossing non-nearest-neighbor partitions of the vertex set $\{1, ..., L_t\}$ with periodic boundary conditions on the set. Now, when $L_t$ is a prime number, all partitions except the partition 1 (i.e., all blocks being singletons) have an $L_t$-fold degeneracy. Therefore,

$$L_t N_{P,tri,PF,L_t} - d_{L_t} = L_t - 1 \quad \text{for prime } L_t \tag{2.1.16}$$

and the theorem follows. □

In [17] it was conjectured that the number $\mathrm{TriCyl}(L_t)$, i.e., $N_{P,tri,PF,L_t}$, behaves asymptotically like $d_{L_t}/L_t$ as $L_t \to \infty$. Our Theorem 3 (2.1.15) proves this conjecture for prime $L_t$.

From eqs. (2.1.12) and (2.1.15), we infer

Table 2: Numbers of $\lambda$'s for the Potts model partition function for the strips of the triangular and square lattices having free and cylindrical boundary conditions and various widths $L_t$.

| $L_t$ | $N_{Z,tri,FF,L_t}$ | $N_{Z,sq,FF,L_t}$ | $2N_{Z,sq,FF,L_t} - N_{Z,tri,FF,L_t}$ | $N_{Z,tri,PF,L_t}$ | $N_{Z,sq,PF,L_t}$ | $2N_{Z,sq,PF,L_t} - N_{Z,tri,PF,L_t}$ | $L_t N_{Z,tri,PF,L_t} - N_{Z,tri,FF,L_t}$ |
|---|---|---|---|---|---|---|---|
| 1 | 1 | 1 | 1 | 1 | 1 | 1 | 0 |
| 2 | 2 | 2 | 2 | 2 | 2 | 2 | 2 |
| 3 | 5 | 4 | 3 | 3 | 3 | 3 | 4 |
| 4 | 14 | 10 | 6 | 6 | 6 | 6 | 10 |
| 5 | 42 | 26 | 10 | 10 | 10 | 10 | 8 |
| 6 | 132 | 76 | 20 | 28 | 24 | 20 | 36 |
| 7 | 429 | 232 | 35 | 63 | 49 | 35 | 12 |
| 8 | 1430 | 750 | 70 | 190 | 130 | 70 | 90 |
| 9 | 4862 | 2494 | 126 | 546 | 336 | 126 | 52 |
| 10 | 16796 | 8524 | 252 | 1708 | 980 | 252 | 284 |
| 11 | 58786 | 29624 | 462 | 5346 | 2904 | 462 | 20 |
| 12 | 208012 | 104468 | 924 | 17428 | 9176 | 924 | 1124 |
| 13 | 742900 | 372308 | 1716 | 57148 | 29432 | 1716 | 24 |

**Conjecture 2** For prime $L_t \geq 3$,

$$N_{P,sq,PF,L_t} = \frac{1}{2}\Big(\frac{d_{L_t}+L_t-1}{L_t} + \frac{1}{4}N_{P,sqtri,FP,\frac{L_t+1}{2}} - \frac{1}{2}R_{\frac{L_t-1}{2}}\Big) \ . \tag{2.1.17}$$

Note that Conjecture 2 is consistent with the conjecture made in [17] that in the limit as $L_t \to \infty$ the ratio $SqCyl(L_t)/TriCyl(L_t) \equiv N_{P,sq,PF,L_t}/N_{P,tri,PF,L_t}$ is equal to 1/2. For non-prime $L_t$, the right-hand sides of eqs. (2.1.15) and (2.1.17) are the lower bounds for $N_{P,tri,PF,L_t}$ and $N_{P,sq,PF,L_t}$, respectively. However, we have not yet obtained formulas for $N_{P,tri,PF,L_t}$ or $N_{P,sq,PF,L_t}$ for arbitrary $L_t$.

## 2.2 $N_{Z,G,BC,L_t}$

Here we carry out a similar analysis for the total number of $\lambda$'s in the Potts model partition function or equivalently, the Tutte polynomial for various lattice strips. First, we list as the left-most column in Table 2 the number of $\lambda$'s that enter in this partition function for the open strip of the triangular lattice of width $L_t$, i.e., $N_{Z,tri,FF,L_t}$. This number is equal to the number of non-crossing partitions of the set $\{1,2,...,L_t\}$, which is precisely the Catalan number. From this observations, it follows that [17]

$$N_{Z,tri,FF,L_t} = C_{L_t} \ . \tag{2.2.1}$$

In the zero-temperature limit for the antiferromagnetic case, one can work in a subspace that corresponds, after a suitable change of basis, to only non-nearest-neighbor partitions [17].

In this limit, the number of $\lambda$'s is thus reduced to the non-crossing, non-nearest-neighbor partitions given by $M_{L_t-1}$ in (2.1.1).

Just as was the case for the chromatic polynomial, the number of $\lambda$'s for the open square-lattice strip with a given width $L_t$ is less than for the open triangular strip of this width because of the symmetry under reflection about the longitudinal axis, which renders some of the partitions equivalent to each other. We proceed to derive this number. Because $2N_{Z,sq,FF,L_t} - N_{Z,tri,FF,L_t}$ gives the number of non-crossing partitions for a slice of the transverse vertices which is symmetric under the reflection symmetry, we have

**Theorem 4**

$$2N_{Z,sq,FF,L_t} - N_{Z,tri,FF,L_t} = \begin{cases} N_{Z,sqtri,FP,\frac{L_t}{2}} & \text{for even } L_t \\ \frac{1}{2} N_{Z,sqtri,FP,\frac{L_t+1}{2}} & \text{for odd } L_t \end{cases} \tag{2.2.2}$$

where $N_{Z,sqtri,FP,L_t}$ was listed in eq. (2.6) from [18].

*Proof* Let us denote $2N_{Z,sq,FF,L_t} - N_{Z,tri,FF,L_t}$ by $Y_{L_t}$ for simplicity, and list, for small $L_t$, the sets $\mathbf{P}_{Y_{L_t}}$ of partitions having reflection symmetry: $\mathbf{P}_{Y_1} = \{1\}$, $\mathbf{P}_{Y_2} = \{1, \delta_{1,2}\}$, $\mathbf{P}_{Y_3} = \{1, \delta_{1,3}, \delta_{1,2,3}\}$, $\mathbf{P}_{Y_4} = \{1, \delta_{2,3}, \delta_{1,4}, \delta_{2,3}\delta_{1,4}, \delta_{1,2}\delta_{3,4}, \delta_{1,2,3,4,5}\}$, $\mathbf{P}_{Y_5} = \{1, \delta_{2,4}, \delta_{1,5}, \delta_{2,4}\delta_{1,5}, \delta_{1,2}\delta_{4,5}, \delta_{2,3,4}, \delta_{1,2,4,5}, \delta_{2,3,4}\delta_{1,5}, \delta_{1,3,5}, \delta_{1,2,3,4,5}\}$. Here it can be seen that going from an odd $L_t$ to $L_t+1$, the number of partitions is doubled because one can split the central vertex to two vertices with or without a delta function for these two vertices. Therefore,

$$Y_{L_t+1} = 2Y_{L_t} \quad \text{for odd } L_t \ . \tag{2.2.3}$$

Going from the partition for an even $L_t$ to the partition for $L_t + 1$, there are two possibilities. The first occurs if there is no delta function connecting any vertex in the vertex set $\{1, 2, .., L_t/2\}$ and the corresponding vertex in vertex set $\{L_t/2 + 1, L_t/2 + 2, .., L_t\}$. Let us denote the number of these kinds of partitions by $Y_{L_t,a}$, which is equal to $N_{Z,tri,FF,L_t/2}$. In this case, one can add a vertex in the middle. The second possibility occurs if there is more than one delta function connecting the two vertex sets mentioned above. Let us denote the number of this kind of partitions by $Y_{L_t,b}$. Clearly $Y_{L_t,a} + Y_{L_t,b} = Y_{L_t}$ for the case of even $L_t$ considered here. For this case one can either add a vertex in the middle without any further delta function or have one more delta function connecting this middle vertex and the nearest vertex pair which are already connected by a delta function. Using eqs. (2.2.1) and (2.2.3), we obtain

$$\begin{aligned} Y_{L_t+1} &= Y_{L_t,a} + 2Y_{L_t,b} && (2.2.4) \\ &= C_{\frac{L_t}{2}} + 2(2Y_{L_t-1} - C_{\frac{L_t}{2}}) && (2.2.5) \\ &= 4Y_{L_t-1} - C_{\frac{L_t}{2}} \quad \text{for even } L_t \ . && (2.2.6) \end{aligned}$$

Set $L_t = 2\ell$ in eq. (2.2.6), we have

$$\begin{aligned} Y_{2\ell+1} &= 4^\ell - 4^{\ell-1}C_1 - 4^{\ell-2}C_2 - ... - C_\ell && (2.2.7) \\ &= \frac{1}{2}\binom{2\ell+2}{\ell+1} && (2.2.8) \\ & && (2.2.9) \end{aligned}$$

and

$$Y_{2\ell} = \binom{2\ell}{\ell} \ . \tag{2.2.10}$$

Using (2.6), this completes the theorem. □

For even $L_t$, $N_{Z,sqtri,FP,\frac{L_t}{2}}$ is equal to the entry in the central column of Pascal's triangle (with rows $r \geq 0$ and elements on the $r$'th row given by $\binom{r}{s}$ for $0 \leq s \leq r$). For odd $L_t$, $(1/2)N_{Z,sqtri,FP,\frac{L_t+1}{2}}$ is equal to the entry in the next-to-central column of this triangle [83].

**Theorem 5**

$$N_{Z,sq,FF,L_t} = \begin{cases} \frac{1}{2}\left[C_{L_t} + \binom{L_t}{\frac{L_t}{2}}\right] & \text{for even } L_t \\ \frac{1}{2}\left[C_{L_t} + \frac{1}{2}\binom{L_t+1}{\frac{L_t+1}{2}}\right] & \text{for odd } L_t \end{cases} \ . \tag{2.2.11}$$

*Proof* The theorem follows from Theorem 4 and eq. (2.2.1). □.

The sequence of numbers $N_{Z,sq,FF,L_t}$ is equal to the number $N_{br,L_t+1}$ of distinct bracelets (i.e. distinct modulo rotations and reflections) with $L_t + 1$ black beads and $L_t$ white beads (given as sequence A007123 in [83] and previously as sequence M1218 in [82]). This can be understood as follows. The number of bracelets enumerated without dividing out by equivalence classes of reflections, i.e. the number that are distinct up to rotations only, with $L_t + 1$ black beads and $L_t$ white beads, is given by the Catalan number $C_{L_t}$. Of these, the number that are symmetric under reflection is $\binom{L_t}{\frac{L_t}{2}}$ for even $L_t$ and $\binom{L_t}{\frac{L_t+1}{2}}$ for odd $L_t$. Therefore, the number of distinct bracelets is the same as the sequence of numbers $N_{Z,sq,FF,L_t}$.

**Corollary 3**

The number $N_{Z,sq,FF,L_t}$ has the leading asymptotic behavior

$$N_{Z,sq,FF,L_t} \sim \frac{1}{2}\pi^{-1/2}L_t^{-3/2}\Big[4^{L_t} + 2^{1/2}L_t 2^{L_t} + O(\frac{1}{L_t})\Big] \quad \text{as} \quad L_t \to \infty \ . \tag{2.2.12}$$

*Proof* This follows from theorem 5 and eq. (2.4). Hence,

**Corollary 4**

$$\lim_{L_t\to\infty} \frac{N_{Z,sq,FF,L_t}}{N_{Z,tri,FF,L_t}} = \frac{1}{2} \ . \tag{2.2.13}$$

*Proof* This follows from (2.2.1) and our new result (2.2.11).

Similarly, consider the quantity $2N_{Z,sq,PF,L_t} - N_{Z,tri,PF,L_t}$ for the strips with cylindrical boundary conditions. We find that this is the same as $2N_{Z,sq,FF,L_t} - N_{Z,tri,FF,L_t}$ for $1 \leq L_t \leq 13$ and infer the following conjecture:

**Conjecture 3** For arbitrary $L_t$,

$$2N_{Z,sq,PF,L_t} - N_{Z,tri,PF,L_t} = \begin{cases} N_{Z,sqtri,FP,\frac{L_t}{2}} & \text{for even } L_t \\ \frac{1}{2}N_{Z,sqtri,FP,\frac{L_t+1}{2}} & \text{for odd } L_t \end{cases} \ . \tag{2.2.14}$$

**Theorem 6**

$$N_{Z,tri,PF,L_t} = \frac{C_{L_t} + 2(L_t - 1)}{L_t} \quad \text{for prime } L_t \ . \tag{2.2.15}$$

*Proof* As shown in [17], $N_{Z,tri,FF,L_t}$ is the number of non-crossing partitions of vertex set $\{1, ..., L_t\}$. Now if $L_t$ is a prime number, except for the partitions 1 (i.e., all blocks being singletons) and $\delta_{1,2,...,L_t}$ (i.e., a unique block), there is an $L_t$-fold degeneracy for the rest of the partitions. Therefore,

$$L_t N_{Z,tri,PF,L_t} - N_{Z,tri,FF,L_t} = 2(L_t - 1) \quad \text{for prime } L_t \tag{2.2.16}$$

and the theorem follows. □

From reference to [83], we observe that the numbers $N_{Z,tri,PF,L_t}$ that we have calculated are equal to the sequence listed as A054357 in [83] which enumerates the number of tree graphs with $L_t$ edges modulo equivalence under 2-coloring (so that, for example, this enumeration includes only one path graph if $L_t$ is odd and includes two path graphs if $L_t$ is even). We also observe that our result (2.2.15) is the special case, for prime $L_t$, of this sequence. A general analytic formula for the above sequence is given in [86]. Based on these connections, we conjecture that

**Conjecture 4** For arbitrary $L_t$

$$N_{Z,tri,PF,L_t} = \frac{1}{L_t}\Big[C_{L_t} + \sum_{d|L_t;\ 1 \le d < L_t} \phi(L_t/d) \binom{2d}{d}\Big] \tag{2.2.17}$$

where $d|L_t$ means that $d$ divides $L_t$ and $\phi(n)$ is the Euler function, equal to the number of positive integers not exceeding the positive integer $n$ and relatively prime to $n$.

Substituting eq. (2.2.17) into eq. (2.2.14) then yields a conjecture for $N_{Z,sq,PF,L_t}$ (again for arbitrary $L_t$), namely

$$N_{Z,sq,PF,L_t} = \begin{cases} \frac{1}{2}\Big[\binom{L_t}{L_t/2} + N_{Z,tri,PF,L_t}\Big] & \text{for even } L_t \\ \frac{1}{2}\Big[\frac{1}{2}\binom{L_t+1}{(L_t+1)/2} + N_{Z,tri,PF,L_t}\Big] & \text{for odd } L_t \ . \end{cases} \tag{2.2.18}$$

where $N_{Z,tri,PF,L_t}$ is given by eq. (2.2.17).

Note that for each strip graphs of a given lattice $\Lambda$ with some specified boundary conditions $BC$ for which one has results from [18], [17] and the present work, the ratio of the number of $\lambda$'s in the chromatic polynomial divided by the number of $\lambda$'s in the full Potts model partition function decreases exponentially fast for $L_t$ and vanishes in the limit of large $L_t$:

$$\lim_{L_t \to \infty} \frac{N_{P,\Lambda,BC,L_t}}{N_{Z,\Lambda,BC,L_t}} = 0 \ . \tag{2.2.19}$$

# 3 Potts Model Partition Functions for Square-lattice Strips with Free Boundary Conditions

The Potts model partition function $Z(G,q,v)$, equivalent to the Tutte polynomial, for a square-lattice strip of width $L_t$ and length $L_\ell = m$ vertices with free boundary conditions is given by

$$Z_{(L_\ell)_{\rm F}\times(L_t)_{\rm F}}(q,v) = \vec{v}^{\rm T}\cdot H\cdot T^{m-1}\cdot\vec{u} \quad (3.1)$$

$$= \vec{w}^{\rm T}\cdot T^{m-1}\cdot\vec{u} \quad (3.2)$$

where $\vec{w}^{\rm T} = \vec{v}^{\rm T}\cdot H$. (No confusion should result between the variable $v$ and the vector $\vec{v}$.) Here $T$ is the transfer matrix, and $H$ is the part of the transfer matrix corresponding to the edges (bonds) lying within a single layer. This partition function was calculated for arbitrary $q$, $v$, and $L_\ell$ with $L_t = 2$ in [12] and with $L_t = 3$ in [13]. It was also calculated for arbitrary $q$ and $v$ for large finite strips in [19]. We review the calculations for arbitrary $L_\ell$ with $L_t = 2, 3$ here in our present notation. We have also calculated the Potts model partition function for arbitrary $L_\ell$ for the strip with widths $L_t = 4$ and $L_t = 5$ having free boundary conditions and have used these for the analyses of partition function zeros given later in this paper, but the results are too lengthy to list here. They are available from the authors on request and in the `mathematica` file `transfer_tutte_sq.m` that is available with the electronic version of this paper in the `cond-mat` archive at `http://www.lanl.gov`.

## 3.1 $L_t = 2$

The number of elements in the basis is trivially equal to two: $\mathbf{P} = \{1, \delta_{1,2}\}$. In this basis, the transfer matrices and the other relevant quantities are given by

$$T = \begin{pmatrix} q^2+3qv+3v^2 & (1+v)(q+2v) \\ v^3 & v^2(1+v) \end{pmatrix} \quad (3.1.1)$$

$$H = \begin{pmatrix} 1 & 0 \\ v & 1+v \end{pmatrix} \quad (3.1.2)$$

$$\vec{v} = \begin{pmatrix} q^2 \\ q \end{pmatrix} \quad (3.1.3)$$

$$\vec{w} = \begin{pmatrix} q(q+v) \\ q(1+v) \end{pmatrix} \quad (3.1.4)$$

$$\vec{u} = \begin{pmatrix} 1 \\ 0 \end{pmatrix} \quad (3.1.5)$$

In [59, 60] a generating function method was presented for chromatic polynomials and was generalized to the full Potts model partition function in [12]. For a strip graph of type $G$, including specification of width and boundary conditions, with arbitrary length $L_\ell = m$,

and denoting the particular member of this class of graphs with length $m$ as $G_m$, one has

$$\Gamma(G,q,v,z) = \sum_{m=0}^{\infty} Z(G_m,q,v) z^m \ . \tag{3.1.6}$$

The generating function is a rational function of the form

$$\Gamma(G,q,v,z) = \frac{\mathcal{N}(G,q,v,z)}{\mathcal{D}(G,q,v,z)} \tag{3.1.7}$$

with

$$\mathcal{N}(G,q,v,z) = \sum_{j=0}^{d_{\mathcal{N}}} A_{G,j}(q,v) z^j \tag{3.1.8}$$

and

$$\mathcal{D}(G,q,v,z) = 1 + \sum_{j=1}^{d_{\mathcal{D}}} b_{G,j}(q,v) z^j \tag{3.1.9}$$

where the $A_{G,j}$ and $b_{G,j}$ are polynomials in $q$ and $v$ that depend on the type of strip (but not its length) of respective degrees $d_{\mathcal{N}}$ and $d_{\mathcal{D}}$ in the auxiliary expansion variable $z$. The factorization of the denominator yields the $\lambda$'s for a given type of strip:

$$\mathcal{D}(G,q,v,z) = \prod_{j=1}^{d_{\mathcal{D}}} (1 - \lambda_{G,j}(q,v) z) \ . \tag{3.1.10}$$

In [59]-[12] a convention was used that allowed for a more general (inhomogeneous) form of strip graph $J(\prod H)I$ in which the end subgraphs $I$ and $J$ could be different from the subgraph $H$ that is repeated to form the strip. Since this generality is not needed for homogeneous lattice strip graphs, a convention was introduced in [15] according to which the $m = 0$ term in the expansion (3.1.6) is taken to be the line graph $T_{L_t}$ rather than a column of squares of height $L_t$. This simplifies the $A_{G,j}$ polynomials in $\mathcal{N}(G,q,v,z)$ (the denominator $\mathcal{D}(G,q,v,z)$ is independent of this convention). Here we shall use the convention of [15]. Further, to shorten the notation, we shall suppress the $G$-dependence on $\mathcal{N}$, $\mathcal{D}$, the $b_{G,j}$, and $A_{G,j}$ where this is obvious. Then for the present strip graph of width $L_t = 2$ [59]

$$\mathcal{D} = 1 + b_1 z + b_2 z^2 \tag{3.1.11}$$

$$\mathcal{N} = A_0 + A_1 z \tag{3.1.12}$$

where [12]

$$b_1 = -(v^3 + 4v^2 + 3qv + q^2) \tag{3.1.13}$$

$$b_2 = v^2(1+v)(q+v)^2 \tag{3.1.14}$$

$$A_0 = v(q+v) \tag{3.1.15}$$

$$A_1 = -q^2 v^2 (1+v) \tag{3.1.16}$$

## 3.2 $L_t = 3$

In this case we have a four-dimensional basis given by $\mathbf{P} = \{1, \delta_{1,2} + \delta_{2,3}, \delta_{1,3}, \delta_{1,2,3}\}$. In this basis the transfer matrix is given by

$$T = \begin{pmatrix} T_{11} & T_{12} & T_{13} & T_{14} \\ v^3(q+2v) & v^2(1+v)(q+3v) & v^3(2+v) & v^2(1+v)^2 \\ v^4 & 2v^3(1+v) & v^2(q+3v+v^2) & v^2(1+v)^2 \\ v^5 & 2v^4(1+v) & v^4(2+v) & v^3(1+v)^2 \end{pmatrix} \tag{3.2.1}$$

where

$$\begin{aligned} T_{11} &= (q+2v)(q^2+3qv+4v^2) && (3.2.2)\\ T_{12} &= 2(1+v)(q^2+4qv+5v^2) && (3.2.3)\\ T_{13} &= q^2+5qv+8v^2+qv^2+3v^3 && (3.2.4)\\ T_{14} &= (1+v)^2(q+3v) && (3.2.5) \end{aligned}$$

The rest of the matrices and vectors are given by

$$\begin{aligned} H &= \begin{pmatrix} 1 & 0 & 0 & 0 \\ v & 1+v & 0 & 0 \\ 0 & 0 & 1 & 0 \\ v^2 & 2v(1+v) & v(2+v) & (1+v)^2 \end{pmatrix} && (3.2.6)\\ \vec{v} &= \begin{pmatrix} q^3 \\ 2q^2 \\ q^2 \\ q \end{pmatrix} && (3.2.7)\\ \vec{w} &= \begin{pmatrix} q(q+v)^2 \\ 2q(1+v)(q+v) \\ q(q+2v+v^2) \\ q(1+v)^2 \end{pmatrix} && (3.2.8)\\ \vec{u} &= \begin{pmatrix} 1 \\ 0 \\ 0 \\ 0 \end{pmatrix} && (3.2.9) \end{aligned}$$

In the generating-function formalism

$$\begin{aligned} \mathcal{D} &= 1 + b_1 z + b_2 z^2 + b_3 z^3 + b_4 z^4 && (3.2.10)\\ \mathcal{N} &= A_0 + A_1 z + A_2 z^2 + A_3 z^3 && (3.2.11) \end{aligned}$$

where

$$b_1 = -q^3 - 5q^2 v - 12qv^2 - 15v^3 - qv^3 - 6v^4 - v^5 \tag{3.2.12}$$

$$
\begin{aligned}
b_2 &= v^2(q+v)(2q^3+13q^2v+q^3v+30qv^2+8q^2v^2+32v^3+21qv^3+q^2v^3 \\
&\quad +30v^4+4qv^4+10v^5+v^6) \qquad (3.2.13)\\
b_3 &= -v^4(1+v)(q+v)^2(q^3+9q^2v+19qv^2+4q^2v^2+15v^3+10qv^3+q^2v^3 \\
&\quad +10v^4+2qv^4+2v^5) \qquad (3.2.14)\\
b_4 &= v^7(1+v)^3(q+v)^5 \qquad (3.2.15)\\
A_0 &= q(q+v)^2 \qquad (3.2.16)\\
A_1 &= -qv^2(-v^4+6q^2v^2+q^2v^3+q^3v+2qv^4+7qv^3+9q^2v+9qv^2+2q^3) \qquad (3.2.17)\\
A_2 &= qv^4(1+v)(q+v)(2qv^3-v^3+q^2v^3+4qv^2+4q^2v^2+7q^2v+q^3) \qquad (3.2.18)\\
A_3 &= -q^3v^7(1+v)^3(q+v)^2 \qquad (3.2.19)
\end{aligned}
$$

# 4 Potts Model Partition Functions for Strips with Cylindrical Boundary Conditions

The Potts model partition function for a square-lattice strip of fixed width $L_t$ vertices and arbitrarily great length $L_\ell = m$ vertices, with cylindrical boundary conditions, is given by

$$
\begin{aligned}
Z_{(L_t)_{\rm P}\times(L_\ell)_{\rm F}}(q;v) &= \vec{v}^{\rm T}\cdot H\cdot T^{m-1}\cdot\vec{u} \qquad (4.1)\\
&= \vec{w}^{\rm T}\cdot T^{m-1}\cdot\vec{u} \qquad (4.2)
\end{aligned}
$$

where $\vec{w}^{\rm T} = \vec{v}^{\rm T}\cdot H$. Here we give results for the cases $L_t = 2$ and $L_t = 3$. We have also calculated this partition function for $L_t = 4, 5$, but the results are too lengthy to list here. They are available from the authors on request and in the `mathematica` file `transfer_tutte_sq.m` that is available with the electronic version of this paper in the `cond-mat` archive at `http://www.lanl.gov`.

## 4.1 $L_t = 2$

The square-lattice strip of width $2_{\rm P}$ is equivalent to the square-lattice strip of width $2_{\rm F}$ when $v = -1$ (chromatic polynomial), but this equivalence does not hold for nonzero temperature. Furthermore, the square-lattice strip of width $2_{\rm P}$ with coupling $v$ is easily seen to be equivalent to an inhomogeneous square-lattice strip of width $2_{\rm F}$ with coupling $v$ in the longitudinal direction and $v' = v(2+v)$ in the transverse direction.

The number of elements in the basis is two: $\mathbf{P} = \{1, \delta_{1,2}\}$. In this basis, the matrices and vectors are given by

$$
\begin{aligned}
T &= \begin{pmatrix} q^2+4qv+5v^2+qv^2+2v^3 & (1+v)^2(q+2v) \\ v^3(2+v) & v^2(1+v)^2 \end{pmatrix} \qquad (4.1.1)\\
H &= \begin{pmatrix} 1 & 0 \\ v(2+v) & (1+v)^2 \end{pmatrix} = \begin{pmatrix} 1 & 0 \\ v & (1+v) \end{pmatrix}^2 \qquad (4.1.2)
\end{aligned}
$$

$$\vec{v} = \begin{pmatrix} q^2 \\ q \end{pmatrix} \tag{4.1.3}$$

$$\vec{w} = \begin{pmatrix} q(q+2v+v^2) \\ q(1+v)^2 \end{pmatrix} \tag{4.1.4}$$

$$\vec{u} = \begin{pmatrix} 1 \\ 0 \end{pmatrix} \tag{4.1.5}$$

In the generating-function language we have

$$\mathcal{D} = 1 + b_1 z + b_2 z^2 \tag{4.1.6}$$

$$\mathcal{N} = A_0 + A_1 z \tag{4.1.7}$$

where

$$b_1 = -(q^2 + 4qv + 6v^2 + qv^2 + 4v^3 + v^4) \tag{4.1.8}$$

$$b_2 = v^2(1+v)^2(q+v)^2 \tag{4.1.9}$$

$$A_0 = q(q + v^2 + 2v) \tag{4.1.10}$$

$$A_1 = -q^2 v^2 (1+v)^2 \tag{4.1.11}$$

## 4.2 $L_t = 3$

For the strip with width $L_t = 3$ and cylindrical boundary conditions (PF3) there are three elements in our basis: $\mathbf{P} = \{1, \delta_{1,2} + \delta_{2,3} + \delta_{1,3}, \delta_{1,2,3}\}$. In this basis the transfer matrix is given by

$$T = \begin{pmatrix} T_{11} & T_{12} & T_{13} \\ v^3(q+4v+v^2) & v^2(1+v)(q+7v+3v^2) & v^2(1+v)^3 \\ v^5(3+v) & 3v^4(1+v)(2+v) & v^3(1+v)^3 \end{pmatrix} \tag{4.2.1}$$

where

$$T_{11} = q^3 + 6q^2 v + 15qv^2 + 16v^3 + qv^3 + 3v^4 \tag{4.2.2}$$

$$T_{12} = 3(1+v)(q^2 + 5qv + 8v^2 + qv^2 + 3v^3) \tag{4.2.3}$$

$$T_{13} = (1+v)^3(q+3v) \tag{4.2.4}$$

The rest of the matrices and vectors are given by

$$H = \begin{pmatrix} 1 & 0 & 0 \\ v & 1+v & 0 \\ v^2(3+v) & 3v(1+v)(2+v) & (1+v)^3 \end{pmatrix} \tag{4.2.5}$$

$$\vec{v} = \begin{pmatrix} q^3 \\ 3q^2 \\ q \end{pmatrix} \tag{4.2.6}$$

$$\vec{w} = \begin{pmatrix} q(q^2+3qv+3v^2+v^3) \\ 3q(1+v)(q+2v+v^2) \\ q(1+v)^3 \end{pmatrix} \tag{4.2.7}$$

$$\vec{u} = \begin{pmatrix} 1 \\ 0 \\ 0 \end{pmatrix} \tag{4.2.8}$$

In the generating-function language we have

$$\mathcal{D} = 1 + b_1 z + b_2 z^2 + b_3 z^3 \tag{4.2.9}$$

$$\mathcal{N} = A_0 + A_1 z + A_2 z^2 \tag{4.2.10}$$

where

$$b_1 = -(q^3+6q^2v+16qv^2+24v^3+2qv^3+16v^4+6v^5+v^6) \tag{4.2.11}$$

$$b_2 = v^2(1+v)(q+v)(q^3+10q^2v+26qv^2+5q^2v^2+24v^3+20qv^3+q^2v^3+26v^4 + 5qv^4+10v^5+v^6) \tag{4.2.12}$$

$$b_3 = -v^5(1+v)^4(q+v)^4 \tag{4.2.13}$$

$$A_0 = q(3v^2+3qv+v^3+q^2) \tag{4.2.14}$$

$$A_1 = -qv^2(1+v)(3qv^4-2v^4+q^2v^3+10qv^3-3v^3+5q^2v^2+9qv^2 + 8q^2v+q^3) \tag{4.2.15}$$

$$A_2 = q^3v^5(1+v)^4(q+v) \tag{4.2.16}$$

# 5 Partition Function Zeros in the $q$ Plane

In this section we shall present results for zeros and the continuous accumulation set (singular locus for the free energy) $\mathcal{B}$ in the $q$ plane for the partition function of the Potts antiferromagnet on square-lattice strips with free longitudinal and free or periodic transverse boundary conditions.

## 5.1 Free Transverse Boundary Conditions

The $L_t = 2$ strip with free boundary conditions was previously studied in [12]. It will be useful to review some of these results. In Fig. 1 we show the accumulation set $\mathcal{B}$ formed by the partition function zeros in the $q$ plane for the Potts antiferromagnet on the free strip of width $L_t = 2$ in the limit of infinite length. For comparison we show the partition function zeros calculated for a finite strip with length $L_\ell = 20$. Evidently, except for obvious discrete zeros such as the zero always present at $q = 0$, these zeros lie close to the asymptotic curves. For $v = -1$, the continuous locus $\mathcal{B} = \emptyset$, with the zeros accumulating at the discrete complex-conjugate points $q = e^{i\pi/3}$. As $v$ increases above $-1$, i.e. the temperature for the Potts antiferromagnet increases above zero, $\mathcal{B}$ forms complex-conjugate arcs whose endpoints

nearest to the real axis approach this axis. As was noted in [12], when $a = e^K = v + 1$ increases through the value $(3/4)^2$, i.e. $v = -7/16$, these endpoints touch the real axis, and in the interval $-7/16 \le v < 0$, $\mathcal{B}$ consists of the above-mentioned complex-conjugate arcs together with a real line segment. As $v \to 0^-$, the locus $\mathcal{B}$ shrinks and finally degenerates to the point at $q = 0$ for $v = 0$ (see Figs. 3,4 in [12]). The ferromagnetic case $1 \le v \le \infty$ has been studied in [12] and will not be discussed here.

Partition functions and zeros in the $q$ plane for finite temperature were previously studied in [19] for the free $L_t = 3$ and $L_t = 4$ strips. In Fig. 2 we show $\mathcal{B}$ in the $q$ plane for the infinite-length limit of the $L_t = 3$ free strip and, for comparison, partition function zeros calculated for a finite strip with length $L_\ell = 30$, for the Potts antiferromagnet. The zeros in this figure are similar to those in Fig. 3.3 in [19]. For zero temperature, i.e., $v = -1$, $\mathcal{B}$ is comprised of the union of a self-conjugate arc passing through $q = 2$ and a complex-conjugate pair of arcs (see Fig. 3(a) in [59]). As the temperature increases above zero, the arcs tend to move together and contract toward the origin. In Fig. 3 we show $\mathcal{B}$ for the infinite-length limit of the free $L_t = 4$ strip and, for comparison, partition function zeros calculated for a finite strip with length $L_\ell = 40$, for the Potts antiferromagnet. The zeros in this figure are similar to those in Fig. 3.9 in [19]. For zero temperature, $\mathcal{B}$ consists of several arcs together with a small real line segment (see Fig. 3(b) in [59]). There are complex-conjugate triple points evident on this locus. Such triple points were studied in [40] in the context of complex-temperature phase diagrams, and it was shown how they arise when curves on the singular locus $\mathcal{B}$ meet in such a manner that, as one travels along given curve(s) past the intersection point the eigenvalues whose degeneracy in magnitude defines the curve cease to be dominant eigenvalues (see Figs. 1 and 2 of [40]). The nature of these triple points was further analyzed in [17]. If one considers $\mathcal{B}$ as the union of the various curves and line segments that comprise it, then a triple point is a multiple point (intersection point) on $\mathcal{B}$, since it lies on multiple branches of $\mathcal{B}$. In a different nomenclature, if one considers each of the algebraic curves comprising $\mathcal{B}$ individually, including the portions where the pairs of degenerate-magnitude $\lambda$'s are not dominant so that these portions are not on $\mathcal{B}$, then such triple points are not multiple points on each individual algebraic curve, since these individual curves pass through the triple point as shown in Fig. 2 in [40]. As was found for the strips with $L_t = 2, 3$, as the temperature increases, the curves forming $\mathcal{B}$ contract toward the origin. One can observe, in particular, that for sufficiently high temperature the triple points disappear.

We proceed to the free strip of width $L_t = 5$. In Fig. 4 we show $\mathcal{B}$ for the infinite-length limit of the free $L_t = 5$ strip and, for comparison, partition function zeros calculated for a finite strip with length $L_\ell = 40$, for the Potts antiferromagnet. The special case $v = -1$ (chromatic polynomial) was studied in [72, 17]. The results exhibit the general trend that for $v = -1$ as $L_t$ increases, the arcs on $\mathcal{B}$ move together, and the endpoints nearest to the origin approach this point. Just as was seen for narrower widths $L_t$, as the temperature increases, the arcs tend to come together further, the prongs protruding to the right contract and eventually disappear, and the entire locus contracts toward the origin. While $\mathcal{B}$ has an oval-like shape for $v = -1$, it becomes more round as $v \to 0^-$.

### 5.2 Periodic Transverse Boundary Conditions

We next consider the strips with cylindrical boundary conditions. In Figs. 5-8 we show $\mathcal{B}$ in the $q$ plane for the infinite-length limits of the cylindrical strips with widths $L_t = 2$ through $L_t = 5$ and partition function zeros on long finite strips of the respective widths, for the Potts antiferromagnet. For the $v = -1$ special case with $L_t = 2, 3$, $\mathcal{B}$ degenerates to discrete points. The $v = -1$ special case for $L_t = 4$ was previously studied in [60] and for $L_t = 5$ in [72, 17] (as well as higher widths in these papers, going up to $L_t = 7$ in [17] and $L_t = 13$ in [75]). The cases $L_t = 3$ and $L_t = 4$ for arbitrary temperature were studied in [19] and our zeros for $L_t = 4$ are similar to those in Fig. 3.12 of [19]. Our present results show that the locus $\mathcal{B}$ tends to become somewhat more complicated as $L_t$ increases.

## 6 Partition Function Zeros in the $v$ Plane

We next present results for complex-temperature (Fisher) zeros and the continuous accumulation set (singular locus for the free energy) $\mathcal{B}$ in the $v$ plane for the partition function of the Potts model on square-lattice strips with free longitudinal boundary conditions and free or periodic transverse boundary conditions. Since the infinite-length limits of the strips considered here are effectively one-dimensional systems and since a one-dimensional spin system with short-range interactions does not have any finite-temperature phase transition, it follows that the locus $\mathcal{B}$ where the free energy is singular does not intersect the real $v$–axis in the interval $-1 < v < \infty$ corresponding to nonzero temperature. Hence there cannot be any physical finite-temperature phase with ferromagnetic or antiferromagnet ordering, and the complex-temperature phase diagram involves only the (complex-temperature extension of the) paramagnetic phase, together with possible O phases, in the nomenclature of [35]. In Fig. 9 we show the Fisher zeros for long finite strips with free boundary conditions, and the approximate respective loci $\mathcal{B}$ for the infinite-length limits of these strips with $L_t$ ranging from 2 through 5. (In Fig. 9(d) the locus $\mathcal{B}$ is shown only for the physical range $\mathrm{Re}(v) \geq -1$.) Corresponding results are presented in Fig. 10 for strips with cylindrical boundary conditions. For each specific width and type of boundary condition we show curves and zeros for $q = 2$, 3, and 4. Although some of these plots are rather complicated, the reader can distinguish the curves for different values of $q$ by their close association with the zeros, which are labelled with different symbols, namely squares, circles, and triangles for $q = 2$, $q = 3$, and $q = 4$, respectively. Furthermore, in the postscript files for the figures in the cond-mat archive, the curves for different $q$ values have different colors: black for $q = 2$, red for $q = 3$, and green for $q = 4$, thereby rendering them easily distinguishable. To complement the types of comparisons that can be made with these plots, we show in Fig. 11 and 12 the loci $\mathcal{B}$ and zeros for various widths plotted together for each value of $q$ from 2 to 4.

There are a number of interesting features that are evident in these plots. In cases where one uses boundary conditions that are self-dual, a subset of the Fisher zeros lie exactly on the circle $|v| = \sqrt{q}$ [23],[24, 26, 20, 77]. It has also been proved [25] that in the limit $q \to \infty$,

$\mathcal{B}$ consists of the unit circle in the complex $\zeta$ plane, where

$$\zeta = \frac{v}{\sqrt{q}} \ . \tag{6.1}$$

Furthermore, the approach to this limit has been studied using exact solutions for $Z(G,q,v)$ on infinite-length, finite-width self-dual strips in [77]. Although the open and cylindrical strip graphs with finite $L_\ell$ used here are not self-dual, in the case of cylindrical boundary conditions, the effect of this non-self-duality is significantly reduced in the limit $L_\ell \to \infty$. Indeed, we find that a subset of the Fisher zeros lie on the respective circles $|v| = \sqrt{q}$, as is evident in the figures. In [23, 24, 26, 19, 20] these zeros were studied for finite slices of the two-dimensional square lattice, and the resultant Fisher zeros form a circular pattern in the $v$ plane which one may infer would become, in the thermodynamic limit, the right-hand boundary of the (complex-temperature extension of the) paramagnetic phase, separating it on the right from the analogous extension of the ferromagnetic phase. Since the Potts model does not have a ferromagnetic phase on the infinite-length finite-width self-dual strip graphs used in [77], what was found there was that the arcs on $\mathcal{B}$ in the $v$ plane end at certain angles that depend on $L_t$ and $q$. Let us introduce polar coordinates for the variable $\zeta$ defined in (6.1): $\zeta = |\zeta|e^{i\theta}$ and denote the value of $\theta$ at the right-hand endpoint of the arc of $\mathcal{B}$ with $|\zeta| = 1$ and $\mathrm{Im}(v) > 0$ as $\theta_{ae}$. For fixed $L_t$, the endpoint angle $\theta_{ae}$ decreases with increasing $q$, and for fixed $q$, $\theta_{ae}$ decreases with increasing $L_t$. Further, for fixed $L_t$, $\lim_{q\to\infty}\theta_{ae} = 0$, and for fixed $q$, $\lim_{L_t\to\infty}\theta_{ae} = 0$ [25, 77]. For our present strips, we find the following results showing the same quantitative trends. For each strip we list three approximate arc endpoint angles corresponding to $q = 2$, $q = 3$, and $q = 4$: for $2_{\rm P} \times \infty_{\rm F}$, $\theta_{ae} \simeq 74^\circ$, $65^\circ$, and $60^\circ$; for $3_{\rm P} \times \infty_{\rm F}$, $\theta_{ae} \simeq 50^\circ$, $40^\circ$, and $35^\circ$; for $4_{\rm P} \times \infty_{\rm F}$, $\theta_{ae} \simeq 38^\circ$, $29^\circ$, and $24^\circ$; and for $5_{\rm P} \times \infty_{\rm F}$, $\theta_{ae} \simeq 31^\circ$, $23^\circ$, and $18^\circ$.

For $q = 2$ in the figure comparing different widths for cylindrical boundary conditions, Fig. 12(a), one can see that the zeros lie not just on the circle $|v| = \sqrt{2}$ but also on the other of the Fisher circles, $|v+2| = \sqrt{2}$, and one can observe how the endpoints on these circles move closer to the real axis as $L_t$ increases. As $L_t \to \infty$, these would then close to produce the full Fisher circles for the model on the infinite square lattice. Finally, for the values $q = 3, 4$, one can observe prongs on the left-most part of $\mathcal{B}$ that are reminiscent of analogous prongs whose endpoints were determined from analyses of low-temperature series expansions for the infinite 2D square lattice in [26].

# 7 Internal Energy and Specific Heat

From the partition function and the resultant reduced free energy for the finite and infinite-length strip, (1.4) and (1.5), it is straightforward to compute the (internal) energy $E$ and specific heat $C$ as

$$E = -\frac{\partial f}{\partial \beta} = -J(v+1)\frac{\partial f}{\partial v} \tag{7.1}$$

and

$$C = \frac{\partial E}{\partial T} = k_B K^2 (v+1) \left[ \frac{\partial f}{\partial v} + (v+1) \frac{\partial^2 f}{\partial v^2} \right] \ . \tag{7.2}$$

In the limit $L_\ell \to \infty$, since only the dominant eigenvalue $\lambda_d$ of the transfer matrix contributes to the free energy, one has

$$f = \frac{1}{L_t} \ln \lambda_d \tag{7.3}$$

$$E = -\frac{J(v+1)}{L_t \lambda_d} \frac{\partial \lambda_d}{\partial v} \tag{7.4}$$

and

$$C = \frac{k_B K^2 (v+1)}{L_t \lambda_d} \left[ (v+1) \frac{\partial^2 \lambda_d}{\partial v^2} - \frac{(v+1)}{\lambda_d} \left( \frac{\partial \lambda_d}{\partial v} \right)^2 + \frac{\partial \lambda_d}{\partial v} \right] \ . \tag{7.5}$$

As noted, since the infinite-length limits of the strips considered here are quasi-one-dimensional systems with free energies that are analytic for all finite temperatures, it follows that the dominant eigenvalue $\lambda_d$ is the same on the whole semi-axis $\mathrm{Im}(v) = 0$, $\mathrm{Re}(v) \geq -1$. Furthermore, as discussed in [12], the free energy and thermodynamic functions such as the internal energy and specific heat for infinite-length finite width lattice strips are independent of the longitudinal boundary conditions (although they depend on the transverse boundary conditions).

For convenience we define a dimensionless internal energy

$$E_r = -\frac{E}{J} = (v+1) \frac{\partial f}{\partial v} \ . \tag{7.6}$$

Note that $\mathrm{sgn}(E_r)$ is (i) opposite to $\mathrm{sgn}(E)$ in the ferromagnetic case where $J > 0$ for which the physical region is $0 \leq v \leq \infty$ and (ii) the same as $\mathrm{sgn}(E)$ in the antiferromagnet case $J < 0$ for which the physical region is $-1 \leq v \leq 0$. We recall the high-temperature (equivalently, small–$|K|$) expansion for an infinite lattice of dimensionality $d \geq 2$ with coordination number $\Delta$:

$$-\frac{E}{J} = E_r = \frac{\Delta}{2} \left[ \frac{1}{q} + \frac{(q-1)K}{q^2} + O(K^3) \right] \ . \tag{7.7}$$

In passing, it should be noted that in papers on the $q = 2$ Ising special case, the Hamiltonian is usually defined as $\mathcal{H}_I = -J_I \sum_{\langle ij \rangle} \sigma_i \sigma_j$ with $\sigma_i = \pm 1$ rather than the Potts model definition (1.2); the isomorphism between these conventions involves the rescaling $2K_I = K$, where $K_I = \beta J_I$. Furthermore, $E_I = -J \langle \sigma_i \sigma_j \rangle$ rather than the Potts definition $E = -J \langle \delta_{\sigma_i \sigma_j} \rangle$, where $\langle ij \rangle$ are adjacent vertices. Hence, for example, for $q = 2$, with the usual Ising model definitions, $E_I(v = 0) = 0$ rather than $E = -J\Delta/(2q)$ and the high-temperature expansion is $E_I = -J(\Delta/2)[K + O(K^3)]$ rather than the $q = 2$ form of (7.7).

We also define the reduced function

$$C_H = \frac{C}{k_B K^2} \ . \tag{7.8}$$

We show in Figures 13–15 the reduced energy $E_r$ and the function $C_H$ that enters in the specific heat for $q = 2$ through $q = 4$ for the square-lattice strips of widths $2 \le L_t \le 5$ with free and cylindrical boundary conditions. We recall that the Potts model on the infinite square lattice has a phase transition from the paramagnetic high-temperature phase in the interval $0 \le v \le v_{p,FM}$ to the low-temperature phase with ferromagnetic long-range order in the interval $v_{p,FM} \le v \le \infty$, where

$$v_{p,FM} = \sqrt{q} \ . \tag{7.9}$$

This phase transition is continous (second-order) for $q \le 4$ and first-order for $q > 4$. In the figures plotting the function $C_H$ entering in the specific heat one can see how the maxima at the respective values of $v \simeq v_{p,FM}$ for various $q$ increase as the width of the strip $L_t$ increases. In the limit $L_t \to \infty$, these maxima diverge, corresponding to the divergence of the specific heat at $v_{p,FM}$. Since the free strips and the cylindrical strips with even $L_t$ are bipartite graphs, there is a well-known isomorphism between the ferromagnetic and antiferromagnetic Ising models, and one sees corresponding maxima at the values of $v$ obtained by the replacement $K \to -K$.

A general property for $E_r$ calculated for the infinite-length limit of the lattice strips with free transverse boundary conditions is that $E = 0$ for $v = -1$, i.e., the zero-temperature limit of the Potts antiferromagnet. This is evident in the figures. For (the infinite-length limit of) the square lattice strips with periodic transverse boundary conditions, the value of $E = 0$ at $v = -1$ for $q \ge \chi$, the chromatic number for these strips, which is 2 if $L_t$ is even and 3 if $L_t$ is odd. For $q = 2$ and $L_t$ odd, there is frustration, and hence $E$ is larger than zero at $v = -1$.

In the limit of infinite temperature on the infinite square lattice, $E_r = 2/q$, as is evident from the expansion (7.7). The infinite-length strips with cylindrical boundary conditions have uniform coordination number $\Delta = 4$, and one sees the agreement with the formula $E_r = 2/q$ in the figures. The infinite-length strips with open boundary conditions do not have a uniform coordination number (this is equal to 3 for the vertices on the upper and lower sides and 4 for the vertices in the interior of the strip). However, one can see the approach to the above formula as $L_t$ increases.

For the $q$-state Potts ferromagnet on the infinite-length finite-width strips with cylindrical boundary conditions, we find that the curves for the energy $E$ cross at a unique value of $v$ depending on $q$ but independent of the width $L_t$; furthermore, this value is equal to the value $v = v_{p,FM}$ at which the phase transition occurs on the infinite square lattice. Let us denote

$$E_p = E(v = v_{p,FM}) \tag{7.10}$$

for the internal energy of the infinite-length finite-width strips evaluated at the value of $v$ given in (7.9). A careful evaluation of the value of $E_p$ reveals that for the range of $q \le 4$ where the Potts ferromagnet on the square lattice has a continuous second-order phase transition, this value is independent of the width $L_t$ and is equal to the value for the infinite square lattice at the ferromagnetic critical point, given by [87]

$$E_c = -J(1 + q^{-1/2}) \ . \tag{7.11}$$

This behavior could have been anticipated in the Ising case, $q = 2$. Finite-size relations for statistical mechanical models using methods of conformal field theory have been discussed in [88]-[92]. For the Ising model, the asymptotic expansion of the internal energy evaluated at $v = v_{p,FM}$ on a torus of length $L_\ell$ and width $L_t$ takes the following form (where we shall use the subscript $c$ to denote the fact that this would be the critical value in two-dimensional thermodynamic limit) [93], [88, 94, 95]

$$E_c(L_t, \rho) = E_c + \sum_{i=0}^{\infty} \frac{E_{2i+1}(\rho)}{(L_t)^{2i+1}} \tag{7.12}$$

where

$$\rho = \frac{L_\ell}{L_t} \tag{7.13}$$

is the aspect ratio of the torus. The infinite-length torus corresponds to the limit $\rho \to \infty$. It has been shown [93, 94, 95] that in this limit

$$E_1(\infty) = E_3(\infty) = E_5(\infty) = 0 \ . \tag{7.14}$$

Furthermore, one can see that all the correction terms have a factor proportional to $\theta_2\theta_3\theta_4$ where $\theta_i$ is the usual $\theta$-function $\theta_i(z, \tau)$ (e.g., [96]) evaluated at $z = 0$, where $\tau = i\rho$, i.e. $q_{nome} \equiv e^{i\tau} = e^{-\pi\rho}$ (see, e.g., Appendix B of [95]). In the limit $\rho \to \infty$, from the basic definitions of these theta functions, it follows that $\theta_2 \to 0$ and $\theta_3, \theta_4 \to 1$. Hence, for the Ising model on an infinitely long cylinder

$$E_c(L_t, \infty) = E_c \tag{7.15}$$

for all widths $L_t$. This (together with the property that the thermodynamic functions are independent of the longitudinal boundary conditions in the limit of infinite length) explains why all of the curves for $E_r$ on the infinite-length, finite-width strips with cylindrical boundary conditions cross at the point $v = v_{p,FM}$ where the the energy attains the critical value on the infinite square lattice, $E_c$. Our numerical results suggest the inference that all the finite-size corrections to the internal energy at the respective ferromagnetic critical points also vanish (for an infinitely long cylinder) for the other two values of $q$, i.e., $q = 3$ and $q = 4$, where the Potts ferromagnet has a second-order phase transition on the infinite square lattice. We have also checked and confirmed that the value of the internal energy at this crossing, $(E_r)_c(v = v_{p,FM})$ is equal to $1 + q^{-1/2}$ for $q > 4$, where the model on the infinite square lattice has a first-order transition, so that the limits of the internal energy at $v = v_{p,FM}$ are different when approached from high and low temperature [87].

Given the bipartite property of the strip graphs with cylindrical boundary conditions and even $L_t$ and the consequent equivalence of the Ising ferromagnet and antiferromagnet, and taking into account our discussion above, it follows that for $q = 2$ the internal energy curves should exhibit a crossing in the antiferromagnetic regime for even $L_t$, and our results agree with this. The point where this occurs is $v = v_{p,AFM} = \sqrt{2} - 2$, and at this point the internal energy is precisely equal to the value on the infinite square lattice, $E_r = 1 - 1/\sqrt{2}$.

Acknowledgment: The research of R.S. was supported in part by the NSF grant PHY-9722101. The research of J. S. was partially supported by CICyT (Spain) grant AEN99-0990. One of us (R.S.) wishes to acknowledge H. Kluepfel for related collaborative work.

# 8 Appendix

In this appendix we recall the connection between the Potts model partition function $Z(G,q,v)$ and the Tutte (also called Tutte/Whitney) polynomial $T(G,x,y)$ for a graph $G=G(V,E)$, given by [5]-[10]

$$T(G,x,y)=\sum_{G'\subseteq G}(x-1)^{k(G')-k(G)}(y-1)^{c(G')} \tag{8.1}$$

where $G'$ is a spanning subgraph of $G$, and $k(G')$, $e(G')$, and $n(G')=n(G)$ denote the number of components, edges, and vertices of $G'$, and

$$c(G')=e(G')+k(G')-n(G') \tag{8.2}$$

is the number of independent circuits in $G'$. As stated in the text, $k(G)=1$ for the graphs of interest here. Now let

$$x=1+\frac{q}{v} \tag{8.3}$$

and

$$y=a=v+1 \tag{8.4}$$

so that

$$q=(x-1)(y-1)\ . \tag{8.5}$$

Then

$$Z(G,q,v)=(x-1)^{k(G)}(y-1)^{n(G)}T(G,x,y)\ . \tag{8.6}$$

For a planar graph $G$ the Tutte polynomial satisfies the duality relation

$$T(G,x,y)=T(G^*,y,x) \tag{8.7}$$

where $G^*$ is the (planar) dual to $G$.

There are several special cases of the Tutte polynomial that are of interest. One that we have commented on in the text and in previous papers is the chromatic polynomial $P(G,q)$. This is obtained by setting $y=0$, i.e., $v=-1$, so that $x=1-q$; the correspondence is $P(G,q)=(-q)^{k(G)}(-1)^{n(G)}T(G,1-q,0)$. A second special case is the flow polynomial [8, 9, 10] $F(G,q)$, obtained by setting $x=0$ and $y=1-q$: $F(G,q)=(-1)^{e(G)-n(G)+k(G)}T(G,0,1-q)$ For planar $G$, given the relation (8.7), the flow polynomial is, up to a power of $q$, proportional to the chromatic polynomial on the dual graph $G$: $F(G,q)\propto P(G^*,q)$. A third special case for $x=1$ is the reliability polynomial (e.g., [9]). Consider a connected graph $G(V,E)$ and now let each edge of $G$ be present with

probability $p$ (and hence absent with probability $1-p$); then the probability that exists a path connecting any two vertices in $G$ is given by the (all-terminal) reliability polynomial $R(G,p) = \sum_{H \subseteq G} p^{e(H)}(1-p)^{e(G)-e(H)}$, where $H$ denotes a connected spanning subgraph of $G$. In turn, this is expressed as a special case of the Tutte polynomial according to

$$R(G,p) = p^{n(G)-1}(1-p)^{e(G)-n(G)+1} T(G, 1, (1-p)^{-1}) \tag{8.8}$$

Thus, our results for $Z(G,q,v)$ and hence, via (8.6), for $T(G,x,y)$ for these lattice strips yield, as a special case, the reliability polynomials for the strips. A conjecture for the complex zeros of the reliability polynomial was given in [97] (see [67] for a recent discussion).

For a given graph $G = (V,E)$, at certain special values of the arguments $x$ and $y$, the Tutte polynomial $T(G,x,y)$ yields quantities of basic graph-theoretic interest [7]-[10]. We recall some definitions: a spanning subgraph was defined at the beginning of the paper; a tree is a connected graph with no cycles; a forest is a graph containing one or more trees; and a spanning tree is a spanning subgraph that is a tree. We recall that the graphs $G$ that we consider are connected. Then the number of spanning trees of $G$, $N_{ST}(G)$, is

$$N_{ST}(G) = T(G,1,1) \ , \tag{8.9}$$

the number of spanning forests of $G$, $N_{SF}(G)$, is

$$N_{SF}(G) = T(G,2,1) \ , \tag{8.10}$$

the number of connected spanning subgraphs of $G$, $N_{CSSG}(G)$, is

$$N_{CSSG}(G) = T(G,1,2) \ , \tag{8.11}$$

and the number of spanning subgraphs of $G$, $N_{SSG}(G)$, is

$$N_{SSG}(G) = T(G,2,2) \ . \tag{8.12}$$

From the duality relation (8.7), one has, for planar graphs $G$ and their planar duals $G^*$,

$$N_{ST}(G) = N_{ST}(G^*) \ , \quad N_{SSG}(G) = N_{SSG}(G^*) \tag{8.13}$$

and

$$N_{SF}(G) = N_{CSSG}(G^*) \ . \tag{8.14}$$

In previous works [12]-[16] we have given resultant formulas for these graphical quantities for the families of graphs considered therein. It is straightforward to do the same for the square-lattice strips considered here. For spanning trees on lattice sections, see also [98, 99].

# References


[1] R. B. Potts, Proc. Camb. Phil. Soc. **48**, 106 (1952).

[2] F. Y. Wu, Rev. Mod. Phys. **54**, 235 (1982).

[3] R. J. Baxter, *Exactly Solved Models in Statistical Mechanics* (Wiley, New York, 1982).

[4] P. W. Kasteleyn and C. M. Fortuin, J. Phys. Soc. Jpn. **26**, 11 (1969) (Suppl.); C. M. Fortuin and P. W. Kasteleyn, Physica **57**, 536 (1972).

[5] W. T. Tutte, Can. J. Math. **6**, 80 (1954).

[6] W. T. Tutte, J. Combin. Theory **2**, 301 (1967).

[7] W. T. Tutte, "Chromials", in Lecture Notes in Math. v. 411 (1974) 243; *Graph Theory*, vol. 21 of Encyclopedia of Mathematics and Applications (Addison-Wesley, Menlo Park, 1984).

[8] N. L. Biggs, *Algebraic Graph Theory* (2nd ed., Cambridge Univ. Press, Cambridge, 1993).

[9] D. J. A. Welsh, *Complexity: Knots, Colourings, and Counting*, London Math. Soc. Lect. Note Ser. 186 (Cambridge University Press, Cambridge, 1993).

[10] B. Bollobás, *Modern Graph Theory* (Springer, New York, 1998).

[11] R. Shrock, in the *Proceedings of the 1999 British Combinatorial Conference, BCC99* (July, 1999), Discrete Math. **231**, 421 (2001).

[12] R. Shrock, Physica A **283**, 388 (2000).

[13] S.-C. Chang and R. Shrock, Physica A **296**, 234 (2001).

[14] S.-C. Chang and R. Shrock, Physica **A 286**, 189 (2000).

[15] S.-C. Chang and R. Shrock, Physica A **296**, 183 (2001).

[16] S.-C. Chang and R. Shrock, Int. J. Mod. Phys. B **15**, 443 (2001).

[17] J. Salas and A. Sokal, J. Stat. Phys., **104**, 609 (2001) (cond-mat/0004330).

[18] S.-C. Chang and R. Shrock, Physica A **296**, 131 (2001).

[19] H. Kluepfel, Stony Brook thesis "The $q$-State Potts Model: Partition Functions and Their Zeros in the Complex Temperature and $q$ Planes" (July, 1999); H. Kluepfel and R. Shrock, unpublished.

[20] S.-Y. Kim and R. Creswick, Phys. Rev. **E63**, 066107 (2001).

[21] M. E. Fisher, *Lectures in Theoretical Physics* (Univ. of Colorado Press, 1965), vol. 7C, p. 1.

[22] P. P. Martin and J. M. Maillard, J. Phys. A **19**, L547 (1986).

[23] P. P. Martin, *Potts Models and Related Problems in Statistical Mechanics* (World Scientific, Singapore, 1991).

[24] C. N. Chen, C. K. Hu, and F. Y. Wu, Phys. Rev. Lett. **76**, 169 (1996).

[25] F. Y. Wu, G. Rollet, H. Y. Huang, J. M. Maillard, C. K. Hu, and C. N. Chen, Phys. Rev. Lett. **76**, 173 (1996).

[26] V. Matveev and R. Shrock, Phys. Rev. **E54**, 6174 (1996).

[27] H. Feldmann, R. Shrock, and S.-H. Tsai, J. Phys. A (Lett.) **30**, L663 (1997); Phys. Rev. **E57**, 1335 (1998).

[28] H. Feldmann, A. J. Guttmann, I. Jensen, R. Shrock, and S.-H. Tsai), J. Phys. A **31**, 2287 (1998).

[29] J. Stephenson and R. Couzens, Physica **129A**, 201 (1984).

[30] W. van Saarloos and D. Kurtze, J. Phys. A **17**, 1301 (1984).

[31] D. Wood, J. Phys. A: Math. Gen. **18**, L481 (1985).

[32] J. Stephenson, J. Phys. A **20**, 4513 (1987).

[33] G. Marchesini and R. Shrock, Nucl. Phys. **B318**, 541 (1989).

[34] R. Abe, T. Dotera, and T. Ogawa, Prog. Theor. Phys. **85**, 509 (1991).

[35] V. Matveev and R. Shrock, J. Phys. A **28**, 1557 (1995).

[36] V. Matveev and R. Shrock, J. Phys. A **28**, 5235 (1995).

[37] V. Matveev and R. Shrock, J. Phys. A **28**, 4859 (1995).

[38] V. Matveev and R. Shrock, Phys. Rev. **E53**, 254 (1996).

[39] V. Matveev and R. Shrock, J. Phys. A **29**, 803 (1996).

[40] V. Matveev and R. Shrock, Phys. Lett. **A221**, 343 (1996).

[41] W. T. Lu and F. Y. Wu, J. Stat. Phys. **102**, 953 (2001).

[42] M. Aizenman and E. H. Lieb, J. Stat. Phys. **24**, 279 (1981).

[43] Y. Chow and F. Y. Wu, Phys. Rev. **B36**, 285 (1987).

[44] R. C. Read, J. Combin. Theory **4**, 52 (1968).

[45] R. C. Read and W. T. Tutte, "Chromatic Polynomials", in *Selected Topics in Graph Theory, 3*, eds. L. W. Beineke and R. J. Wilson (Academic Press, New York, 1988.).

[46] A. Lenard, calculation of $W(sq, q = 3) = (4/3)^{3/2}$ (unpublished), cited in Ref. [47].

[47] E. H. Lieb, Phys. Rev. **162**, 162 (1967).

[48] R. J. Baxter, J. Math. Phys. **11**, 784 (1970).

[49] N. L. Biggs, R. M. Damerell, and D. A. Sands, J. Combin. Theory B **12**, 123 (1972).

[50] N. L. Biggs and G. H. Meredith, J. Combin. Theory B**20**, 5 (1976).

[51] N. L. Biggs, Bull. London Math. Soc. **9**, 54 (1976).

[52] S. Beraha, J. Kahane, and N. Weiss, J. Combin. Theory B **27**, 1 (1979); *ibid.* **28**, 52 (1980).

[53] R. J. Baxter, J. Phys. A **20**, 5241 (1987).

[54] R. C. Read and G. F. Royle, in *Graph Theory, Combinatorics, and Applications* (Wiley, NY, 1991), vol. 2, p. 1009.

[55] J. Salas and A. Sokal, J. Stat. Phys. **86**, 551 (1997).

[56] R. Shrock and S.-H. Tsai, Phys. Rev. **E55**, 5165 (1997).

[57] R. Shrock and S.-H. Tsai, Phys. Rev. **E56**, 1342, 2733, 3935, 4111 (1997).

[58] R. Shrock and S.-H. Tsai, Phys. Rev. **E58**, 4332 (1998); cond-mat/9808057.

[59] M. Roček, R. Shrock, and S.-H. Tsai, Physica **A252**, 505 (1998).

[60] M. Roček, R. Shrock, and S.-H. Tsai, Physica **A259**, 367 (1998).

[61] R. Shrock and S.-H. Tsai, Physica **A259**, 315 (1998).

[62] R. Shrock and S.-H. Tsai, J. Phys. A **31**, 9641 (1998); Physica **A265** (1999) 186.

[63] R. Shrock and S.-H. Tsai, J. Phys. A Lett. **32**, L195 (1999).

[64] R. Shrock and S.-H. Tsai, Phys. Rev. **E60**, 3512 (1999).

[65] R. Shrock and S.-H. Tsai, Physica A **275**, 429 (1999).

[66] R. Shrock and S.-H. Tsai, J. Phys. **32**, 5053 (1999).

[67] A. Sokal, Comb. Probab. Comput. **10**, 41 (2001).

[68] N. L. Biggs, J. Combin. Theory B **82**, 19 (2001); Bull. London Math. Soc., in press.

[69] R. Shrock, Phys. Lett. **A261**, 57 (1999).

[70] N. L. Biggs and R. Shrock, J. Phys. A (Letts) **32**, L489 (1999).

[71] S.-C. Chang and R. Shrock, Phys. Rev. **E 62**, 4650 (2000).

[72] S.-C. Chang and R. Shrock, Physica A **290**, 402 (2001).

[73] S.-C. Chang and R. Shrock, Physica A **292**, 307 (2001).

[74] S.-C. Chang and R. Shrock, Ann. Phys. **290**, 124 (2001).

[75] J. L. Jacobsen and J. Salas, J. Stat. Phys. **104**, 701 (2001) (cond-mat/0011456).

[76] J. Salas and R. Shrock, Phys. Rev. E **64**, 011111 (2001) (cond-mat/0002190).

[77] S.-C. Chang and R. Shrock, Physica A **301**, 301 (2001); Phys. Rev. E **64**, 066116 (2001).

[78] T. Motzkin, Bull. Amer. Math. Soc. **54**, 352 (1948).

[79] R. Donaghey and L. W. Shapiro, J. Combin. Theory, A **23**, 291 (1977).

[80] M. Aigner, Europ. J. Combin. **19**, 663 (1998).

[81] R. P. Stanley, *Enumerative Combinatorics* (Cambridge University Press, Cambridge, 1999), v. 2.

[82] N. J. A. Sloane and S. Plouffe, *The Encyclopedia of Integer Sequences* (Academic Press, New York, 1995).

[83] N. J. A. Sloane, *The On-Line Encyclopedia of Integer Sequences*, `http://www.research.att.com/~njas/sequences/` .

[84] F. R. Bernhart, Disc. Math. **204**, 73 (1999).

[85] In the equation for $R_n$ given in [17] the lower limit of the summation should be 1 rather than 0.

[86] M. Bona, M. Bousquet, G. Labelle, and P. Leroux, Adv. in Appl. Math. **24**, 22 (2000) (math.CO/9804119).

[87] For completeness, we recall that [2, 3] for $q > 4$, $\lim_{v \nearrow v_{p,FM}} E_r = (1 + q^{-1/2})[1 - D(q)\tanh(\mu/2)]$ and $\lim_{v \searrow v_{p,FM}} E_r = (1 + q^{-1/2})[1 + D(q)\tanh(\mu/2)]$ where $\mu = \mathrm{arccosh}(q^{1/2}/2)$ and $D(q) = \prod_{n=1}^{\infty}(\tanh(n\mu))^2$. For the Potts model on the infinite-length, finite-width strips, this discontinuity is absent.

[88] J. L. Cardy, J. Phys. A **17**, L385, L961 (1984); H. W. J. Blöte, and M. P. Nightingale, Phys. Rev. Lett. **56**, 742 (1986); I. Affleck, Phys. Rev. Lett. **56**, 746 (1986).

[89] H. Park and M. den Nijs, Phys. Rev. B **38**, 565 (1988).

[90] J. Cardy, in C. Domb and J. L. Lebowitz, eds., *Phase Transitions and Critical Phenomena* (Academic Press, New York, 1987), vol. 11, p. 55.

[91] V. Privman, P. C. Hohenberg, and A. Aharony, in in C. Domb and J. L. Lebowitz, eds., *Phase Transitions and Critical Phenomena* (Academic Press, New York, 1987), vol. 14, p. 1.

[92] P. Di Francesco, P. Mathieu, and D. Sénéchal, *Conformal Field Theory* (Springer, New York, 1997).

[93] A. Ferdinand and M.E. Fisher, Phys. Rev. **185**, 832 (1969).

[94] N. Izmailian and C.-K. Hu, cond-mat/0009024.

[95] J. Salas, J. Phys. A **34**, 1311 (2001).

[96] M. Abramowitz and I. Stegun, *Handbook of Mathematical Functions* (Dover, New York, 1965).

[97] J. Brown and C. Colbourn, SIAM J. Discrete Math. **5**, 571 (1992).

[98] W. Tzeng and F. Y. Wu, Lett. Appl. Math. **13**, 19 (2000).

[99] R. Shrock and F. Y. Wu, J. Phys. A **33**, 3881 (2000).

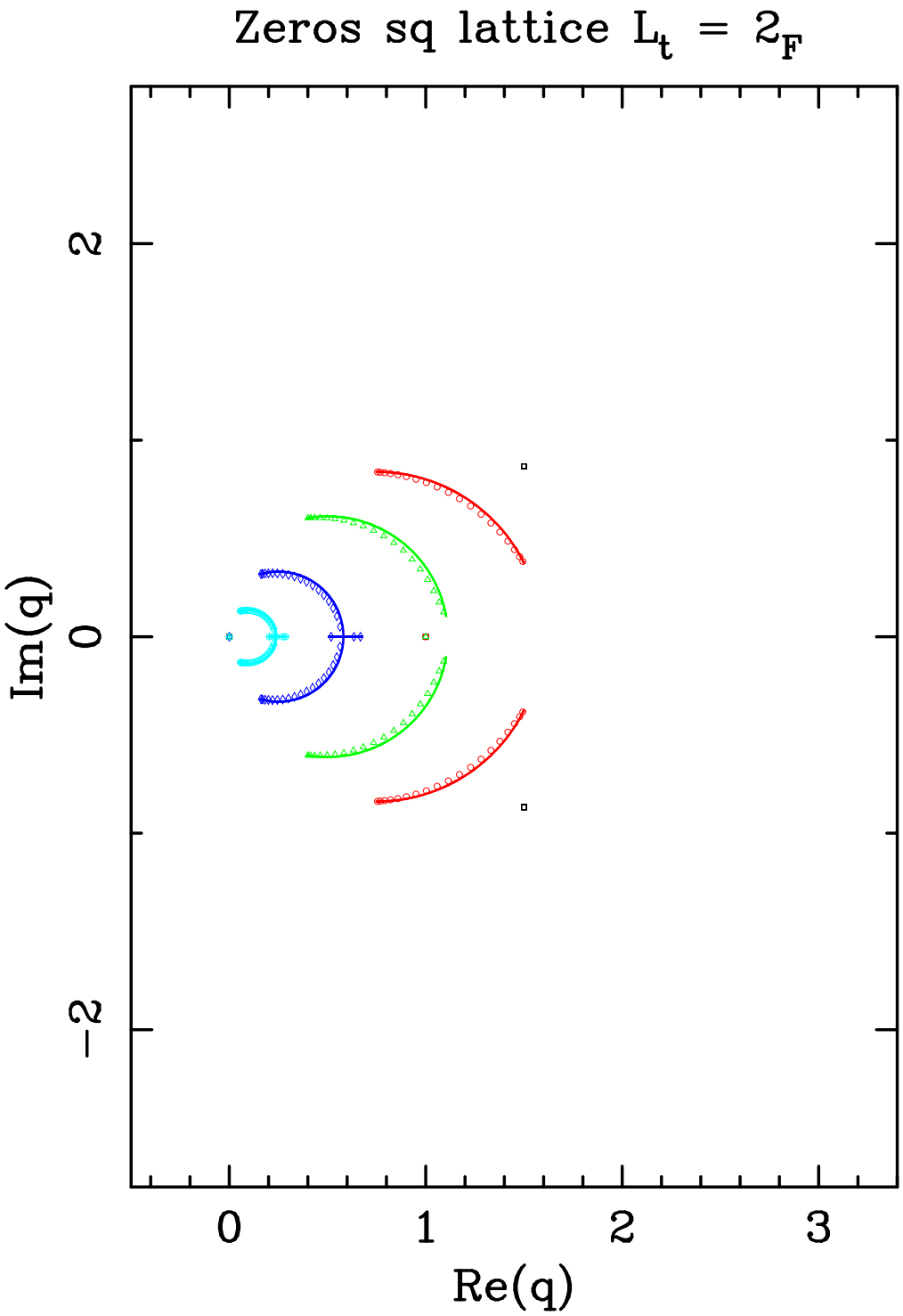


Figure 1: Partition-function zeros in the complex $q$ plane for the $2_F \times 20_F$ square-lattice strip and resultant accumulation set $\mathcal{B}$ for the $2_F \times \infty_F$ strip (singular locus for the free energy) for several values of the temperature-like parameter $v$: $-1$ ($\Box$), $-0.75$ ($\circ$), $-0.50$ ($\triangle$), $-0.25$ ($\diamond$), and $-0.10$ ($\oplus$), where the symbols correspond to the zeros calculated for the finite strip. The zero at $q = 0$ is present for all $v$.

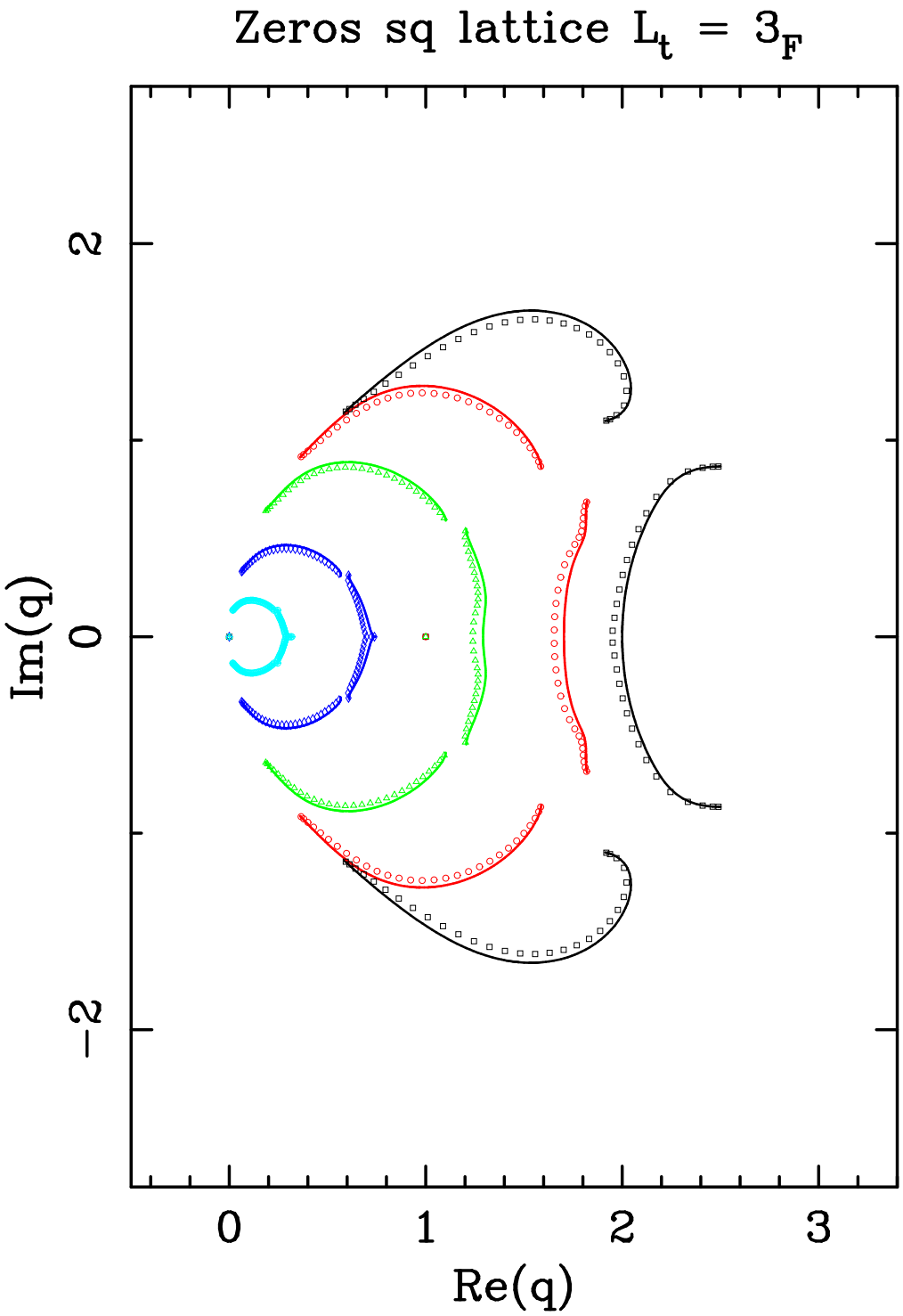


Figure 2: Partition-function zeros in the complex $q$ plane for the $3_F \times 30_F$ square-lattice strip for several values of the temperature-like parameter $v$: $-1$ ($\Box$), $-0.75$ ($\circ$), $-0.50$ ($\triangle$), $-0.25$ ($\diamond$), and $-0.10$ ($\oplus$). The loci $\mathcal{B}$ for the $3_F \times \infty_F$ strip for these values of $v$ are also shown.

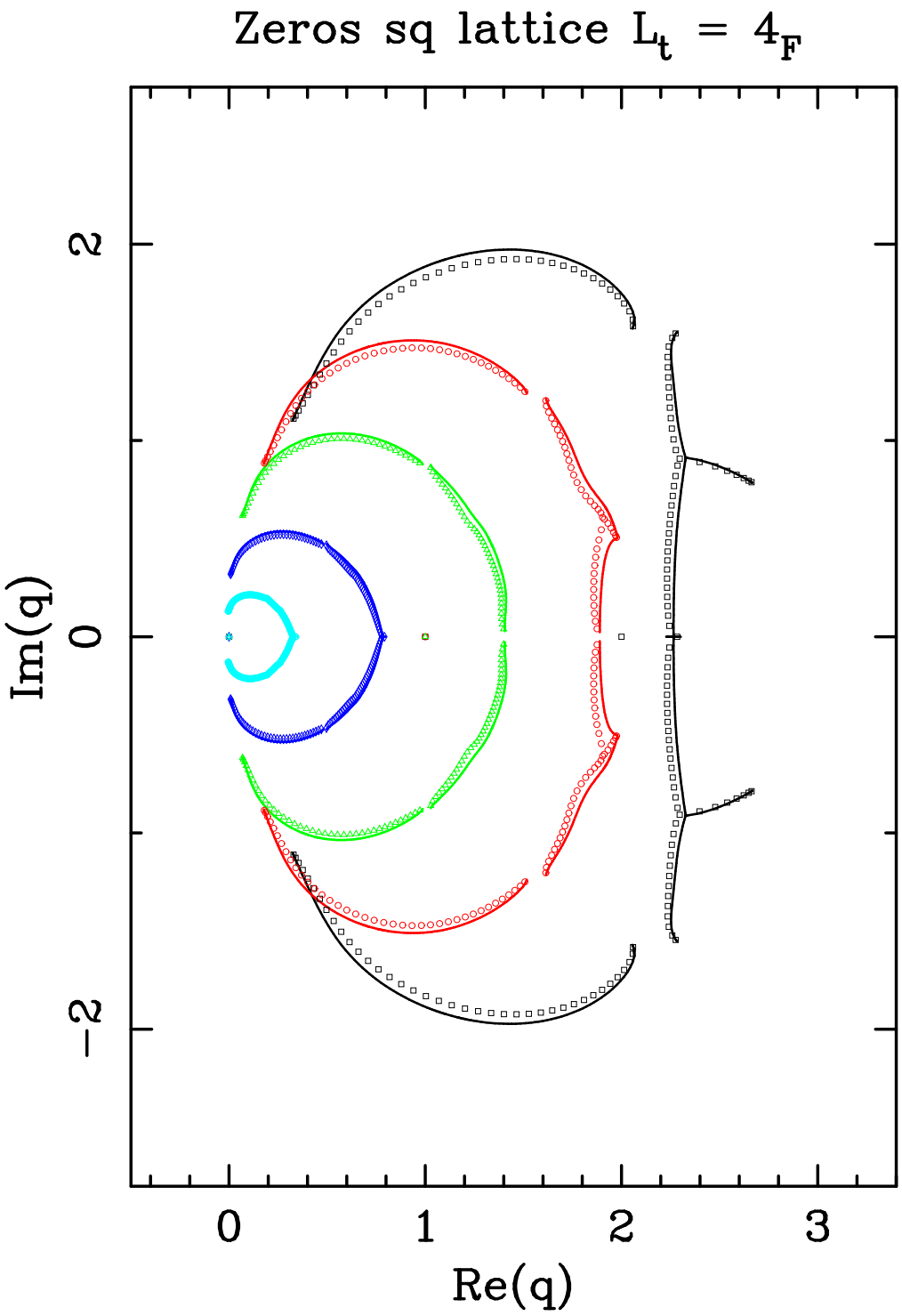


Figure 3: Partition-function zeros in the complex $q$ plane for the for the $4_F \times 40_F$ strip for several values of the temperature-like parameter $v$: $-1$ ($\Box$), $-0.75$ ($\circ$), $-0.50$ ($\triangle$), $-0.25$ ($\diamond$), and $-0.10$ ($\oplus$). The loci $\mathcal{B}$ for the $4_F \times \infty_F$ strip for these values of $v$ are also shown.

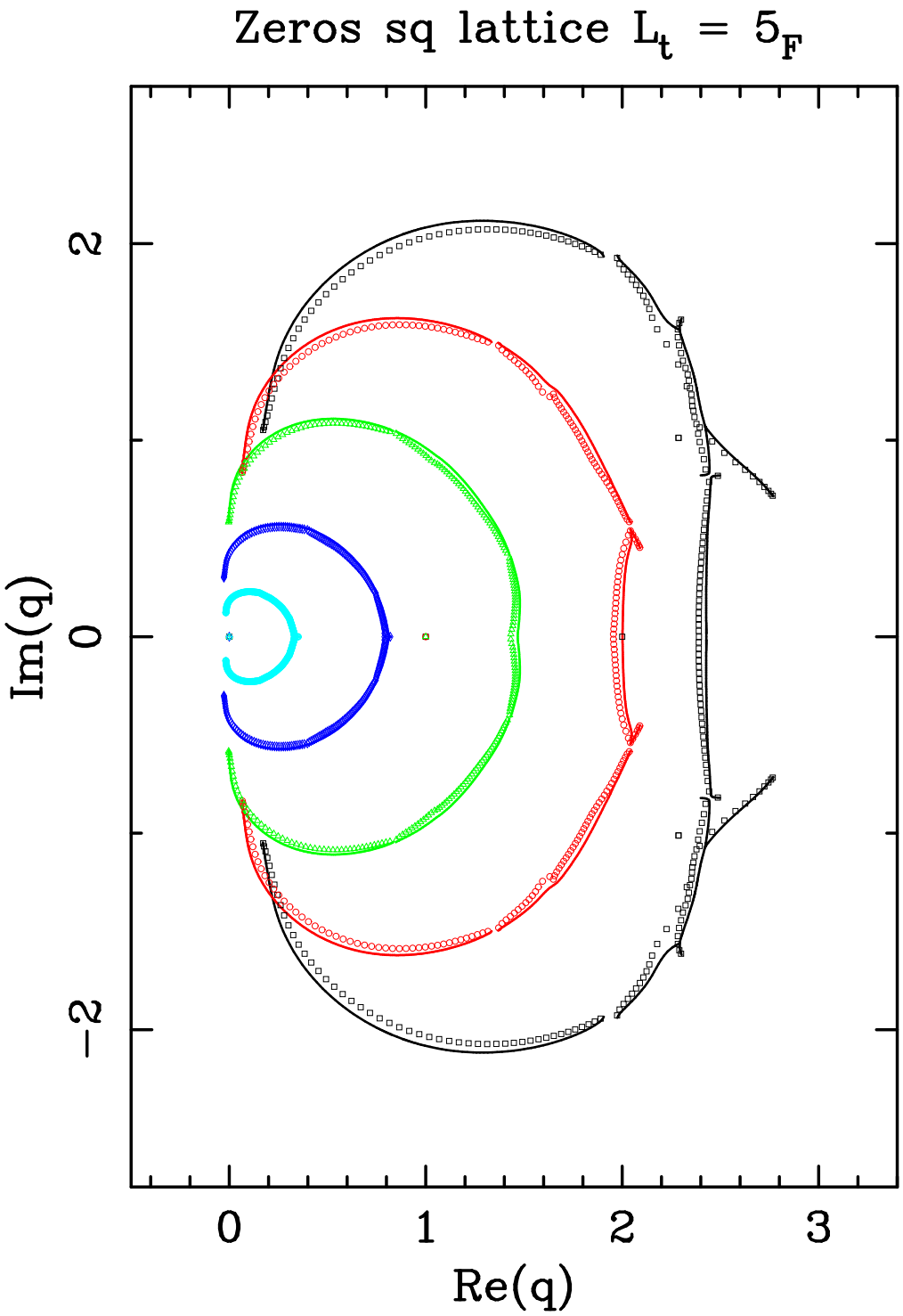


Figure 4: Partition-function zeros in the complex $q$ plane for the $5_{\rm F} \times 40_{\rm F}$ square-lattice strip for several values of the temperature-like parameter $v$: $-1$ ($\Box$), $-0.75$ ($\circ$), $-0.50$ ($\triangle$), $-0.25$ ($\diamond$), and $-0.10$ ($\oplus$). The loci $\mathcal{B}$ for the $5_{\rm F} \times \infty_{\rm F}$ strip for these values of $v$ are also shown.

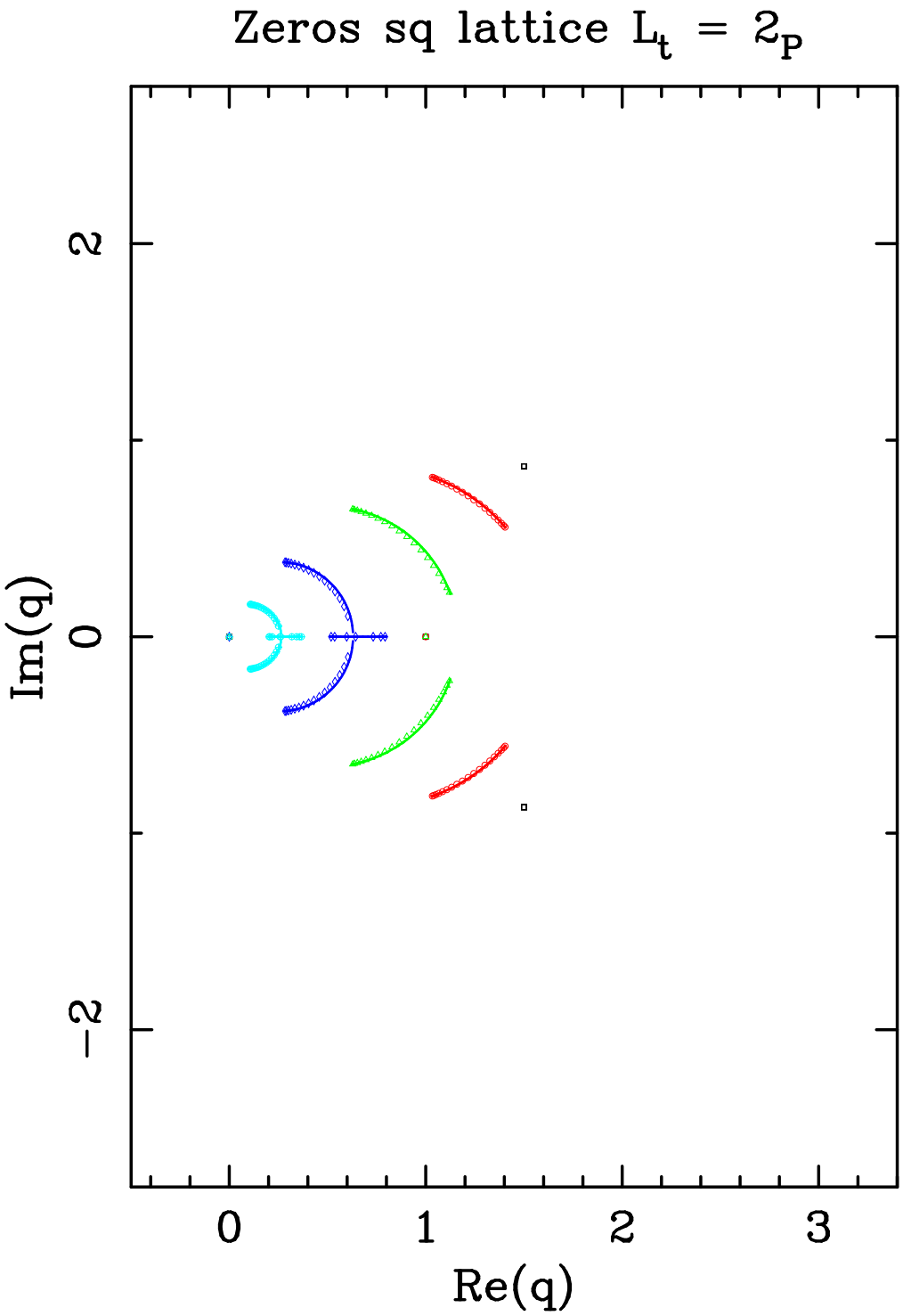


Figure 5: Partition-function zeros in the complex $q$ plane for the $2_{\rm P} \times 20_{\rm F}$ square-lattice strip for several values of the temperature-like parameter $v$: $-1$ ($\Box$), $-0.75$ ($\circ$), $-0.50$ ($\triangle$), $-0.25$ ($\diamond$), and $-0.10$ ($\oplus$). The loci $\mathcal{B}$ for the $2_{\rm P} \times \infty_{\rm F}$ strip for these values of $v$ are also shown.

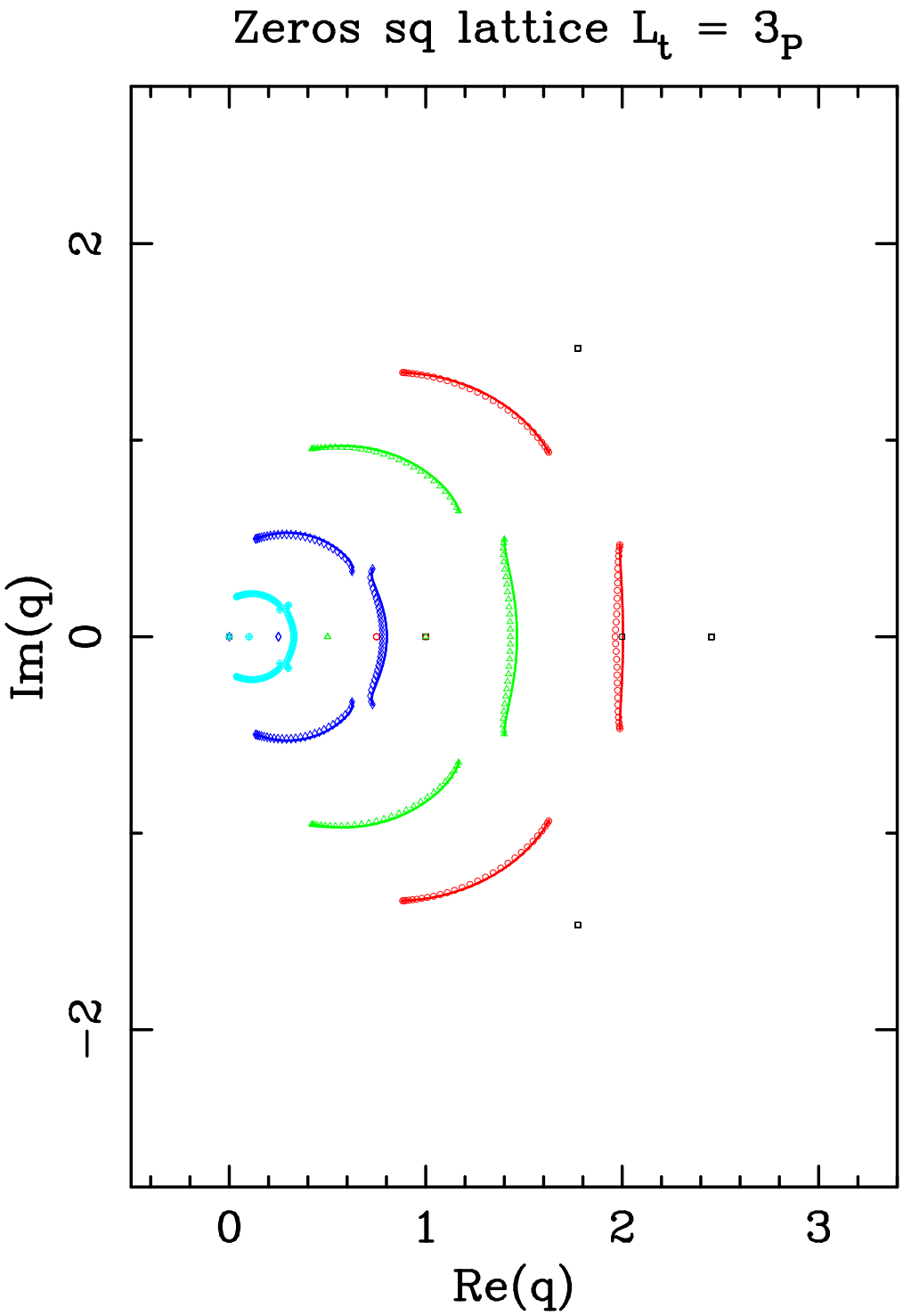


Figure 6: Partition-function zeros in the complex $q$ plane for the $3_{\rm P} \times 30_{\rm F}$ square-lattice strip for several values of the temperature-like parameter $v$: $-1$ ($\Box$), $-0.75$ ($\circ$), $-0.50$ ($\triangle$), $-0.25$ ($\diamond$), and $-0.10$ ($\oplus$). The loci $\mathcal{B}$ for the $3_{\rm P} \times \infty_{\rm F}$ strip for these values of $v$ are also shown.

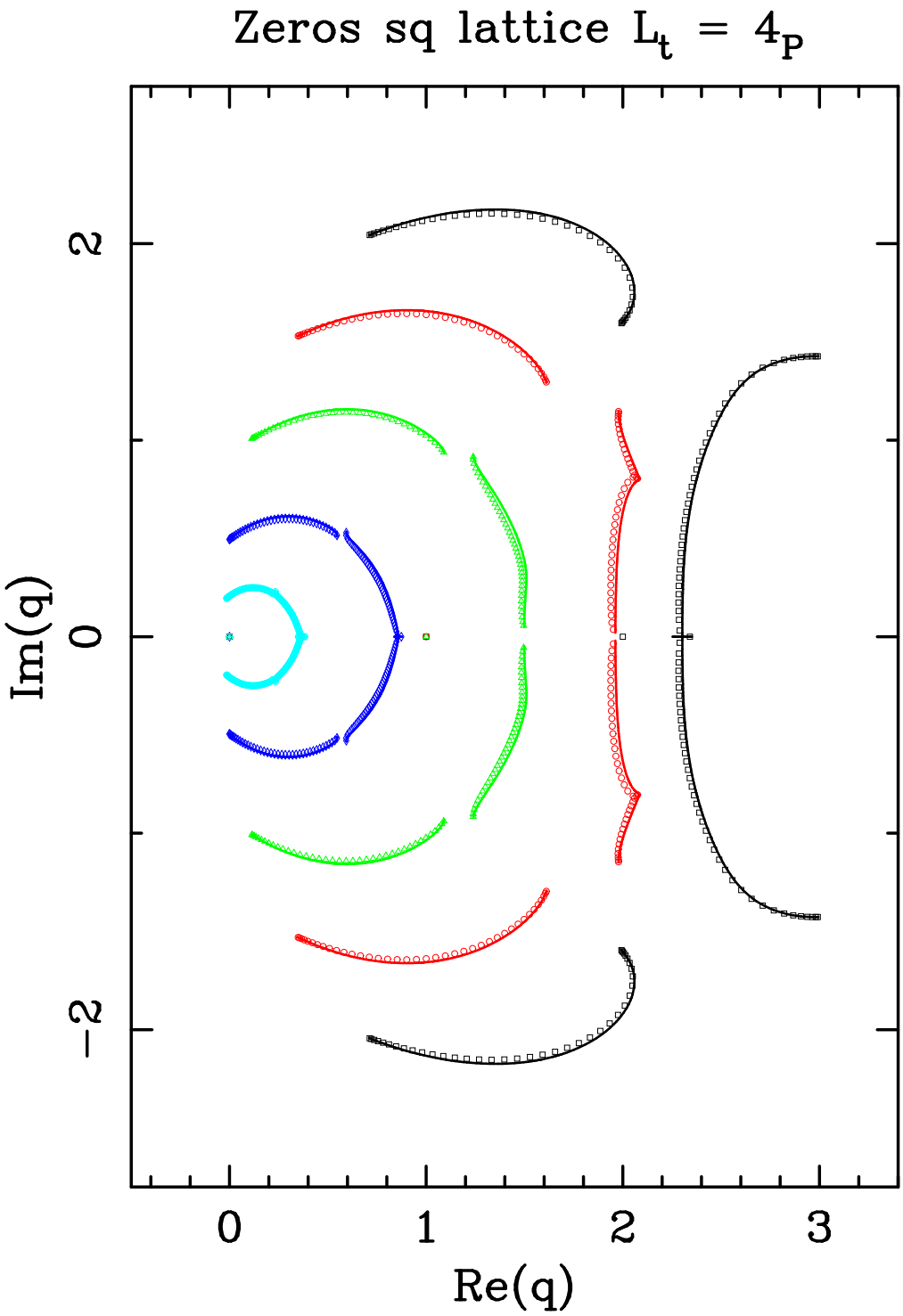


Figure 7: Partition-function zeros in the complex $q$ plane for the $4_{\rm P} \times 40_{\rm F}$ square-lattice strip for several values of the temperature-like parameter $v$: $-1$ ($\Box$), $-0.75$ ($\circ$), $-0.50$ ($\triangle$), $-0.25$ ($\diamond$), and $-0.10$ ($\oplus$). The loci $\mathcal{B}$ for the $4_{\rm P} \times \infty_{\rm F}$ strip for these values of $v$ are also shown.

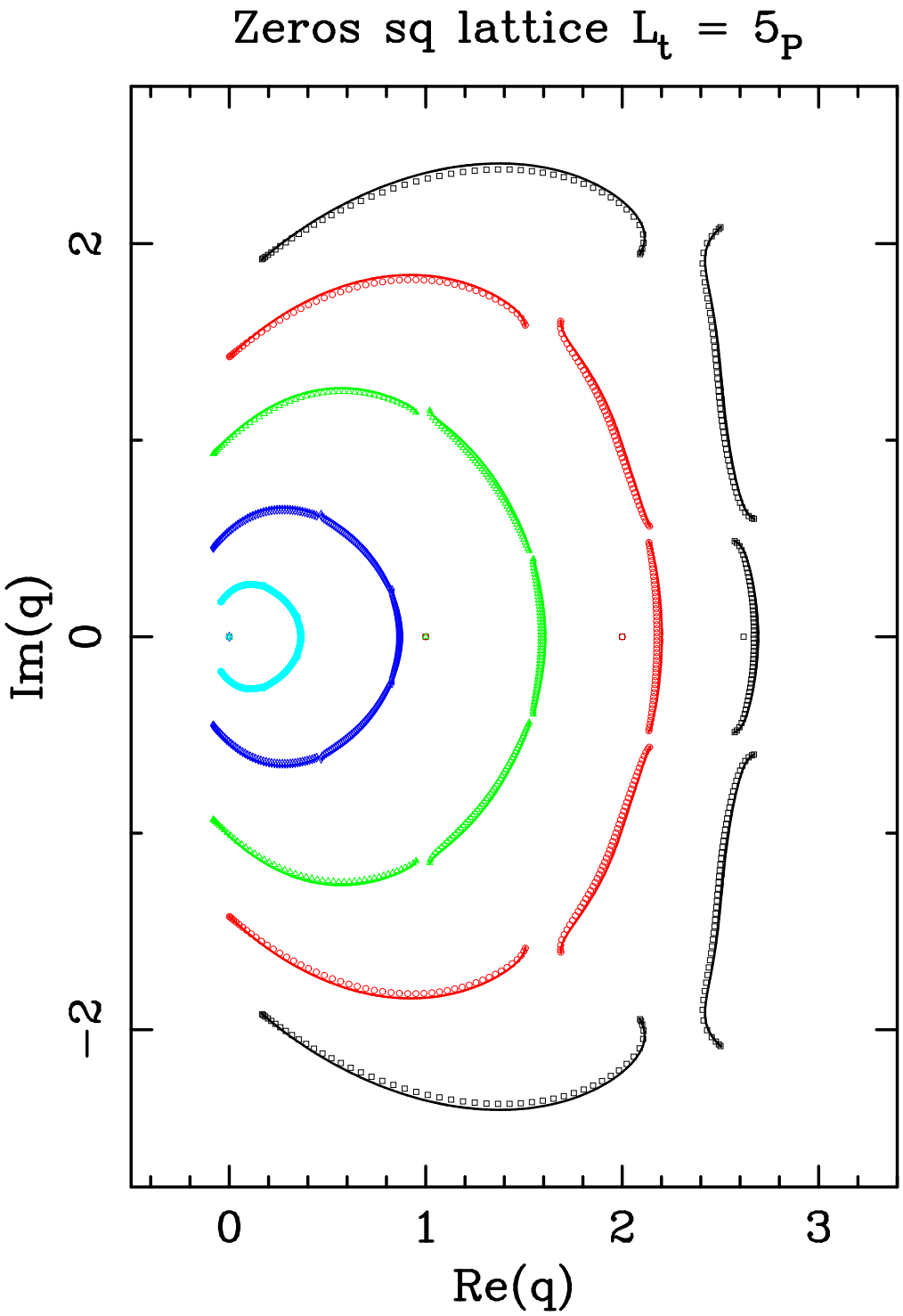


Figure 8: Partition-function zeros in the complex $q$ plane for the $5_{\rm P} \times 40_{\rm F}$ square-lattice strip for several values of the temperature-like parameter $v$: $-1$ ($\Box$), $-0.75$ ($\circ$), $-0.50$ ($\triangle$), $-0.25$ ($\diamond$), and $-0.10$ ($\oplus$). The loci $\mathcal{B}$ for the $5_{\rm P} \times \infty_{\rm F}$ strip for these values of $v$ are also shown.

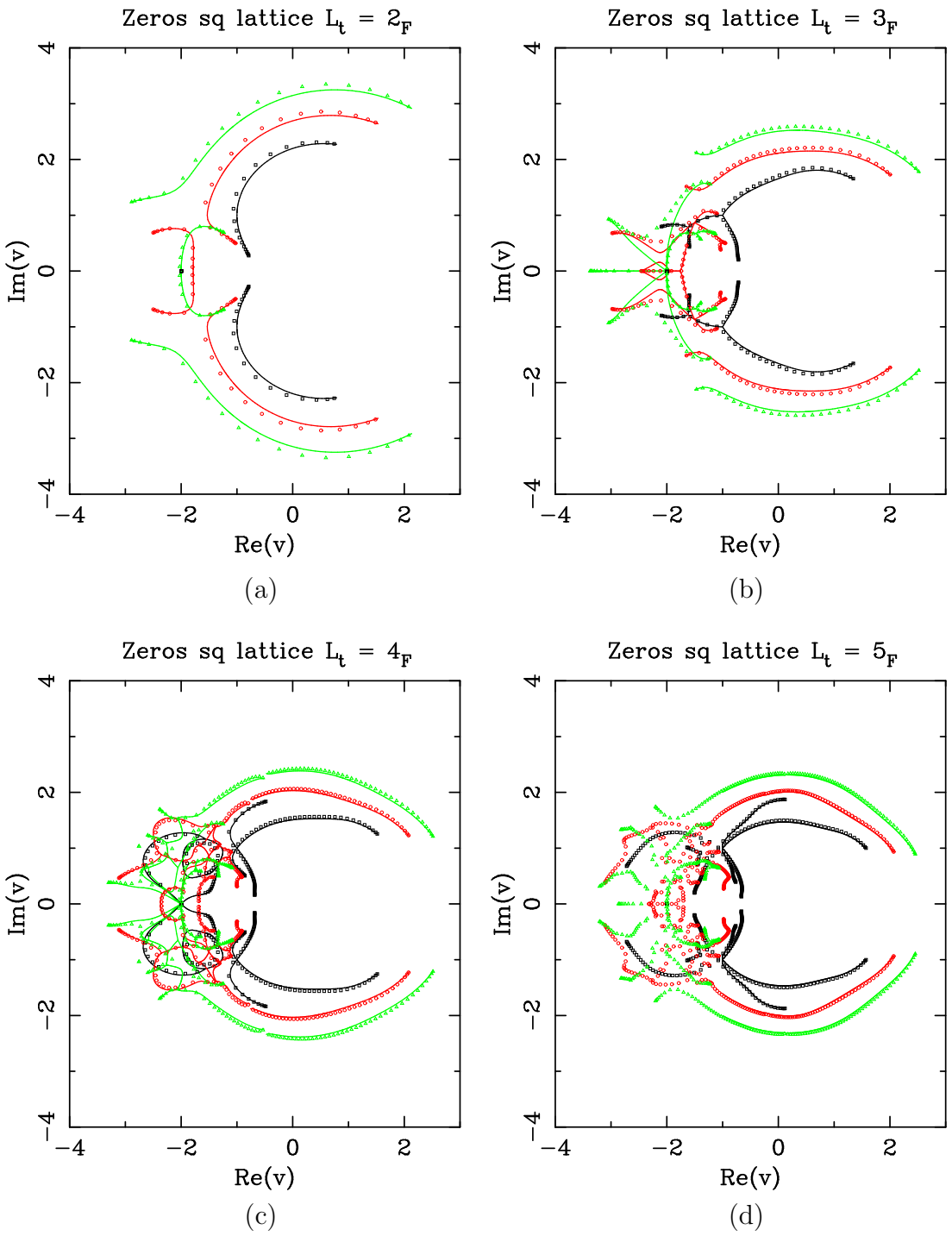


Figure 9: Partition function zeros in the complex $v$ plane for several square-lattice strips: (a) $2_F \times 20_F$, (b) $3_F \times 30_F$, (c) $4_F \times 40_F$, and (d) $5_F \times 50_F$. In each plot we show the zeros for several values of the parameter $q$: 2 (□, black), 3 (○, red), and 4 (△, green) and the corresponding loci $\mathcal{B}$ for these values of $q$.

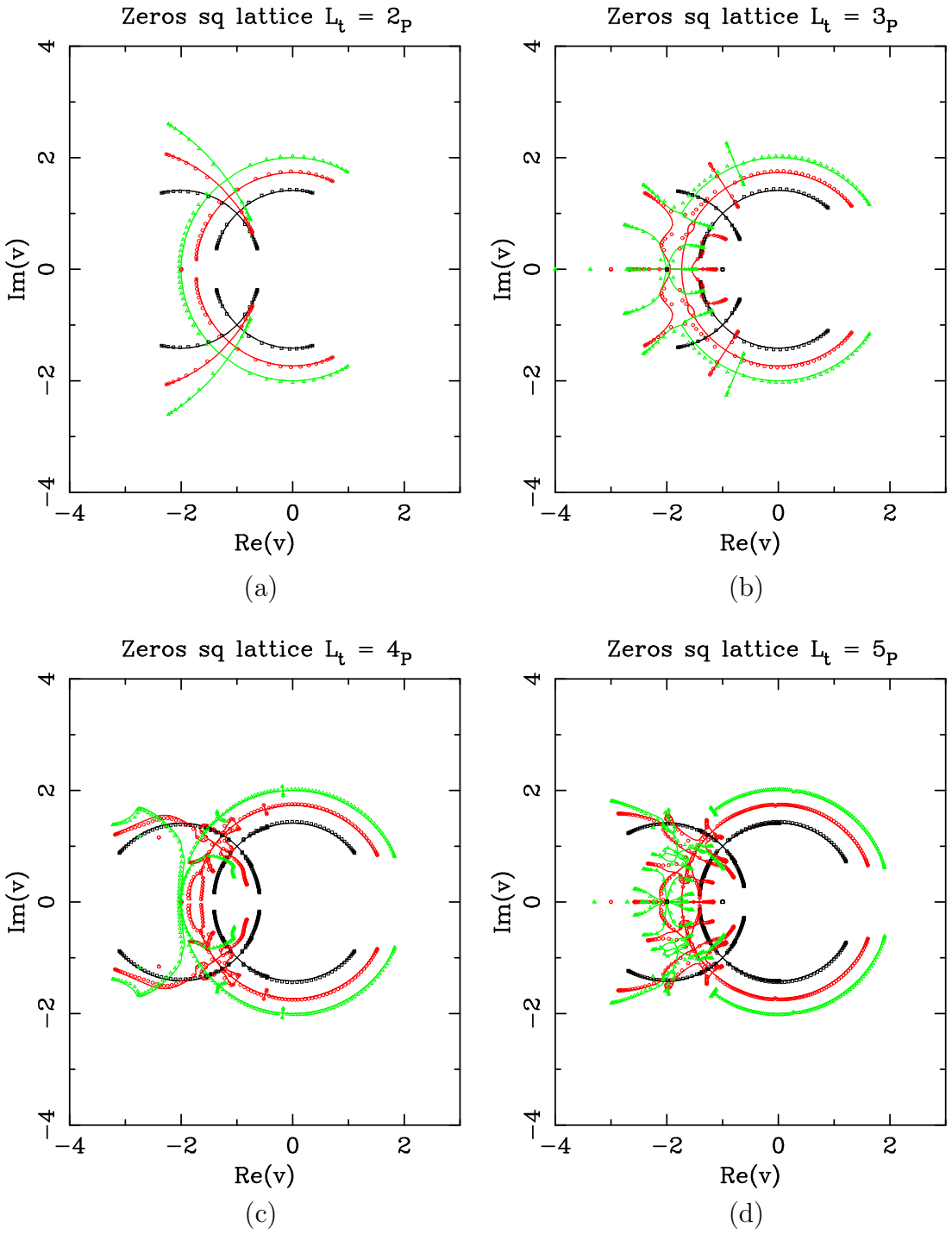


Figure 10: Partition function zeros in the complex $v$ plane for several square-lattice strips: (a) $2_P \times 20_F$, (b) $3_P \times 30_F$, (c) $4_P \times 40_F$, and (d) $5_P \times 50_F$. In each plot we show the zeros for several values of the parameter $q$: 2 (□, black), 3 (○, red), and 4 (△, green) and the corresponding loci $\mathcal{B}$ for these values of $q$.

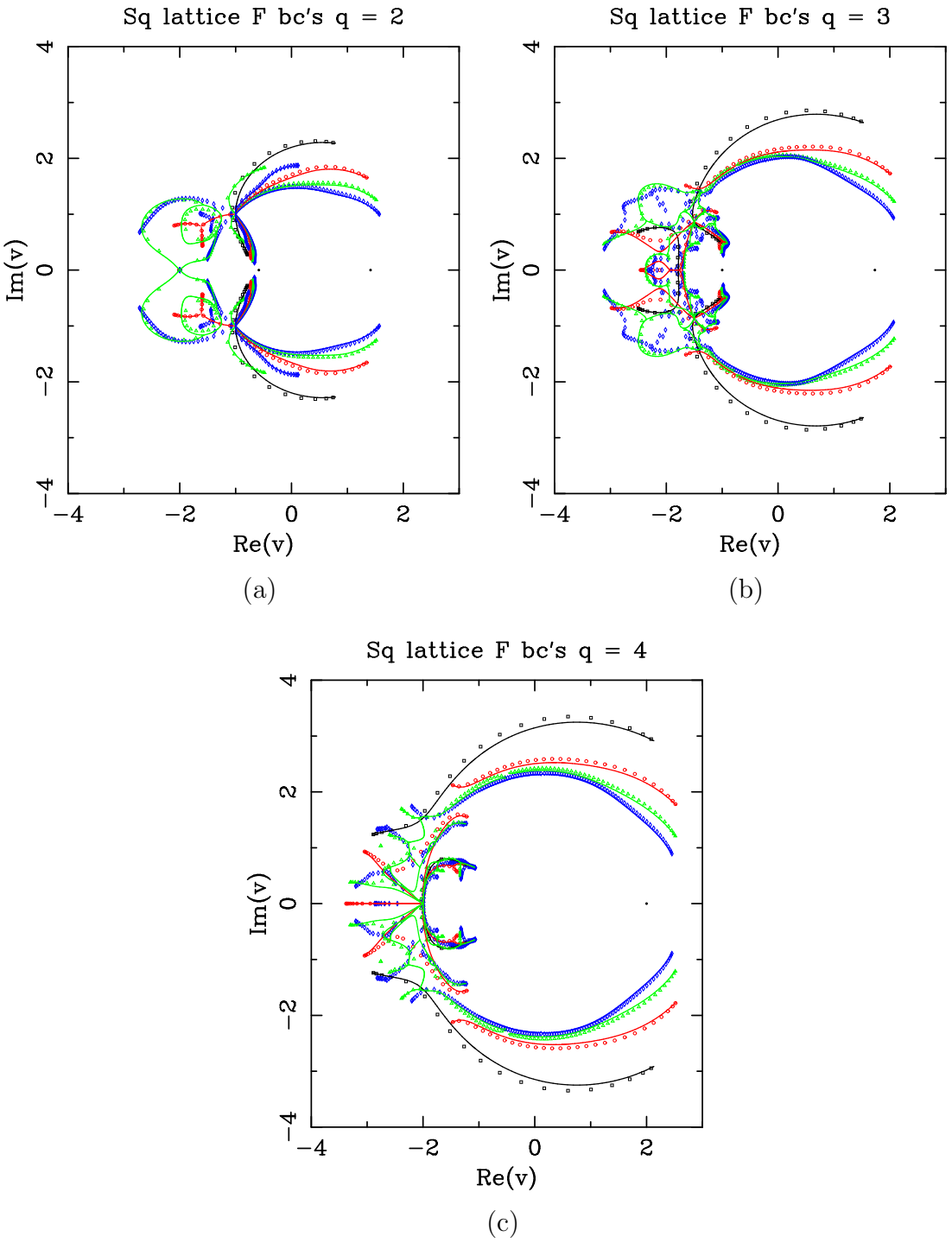


Figure 11: Limiting curves forming the singular locus $\mathcal{B}$, in the $v$ plane, for the free energy of the $q = 2$ (a) $q = 3$ (b), and $q = 4$ (c) Potts model on the $(L_t)_{\rm F} \times \infty_{\rm F}$ square-lattice strips with the following widths $L_t$: 2 (black), 3 (red), 4 (green), and 5 (blue). We also show the partition-function zeros for the strips $(L_t)_{\rm F} \times (10L_t)_{\rm F}$ for the same values of $L_t$: 2 ($\Box$, black), 3 ($\circ$, red), 4 ($\triangle$, green), and 5 ($\diamond$, blue).

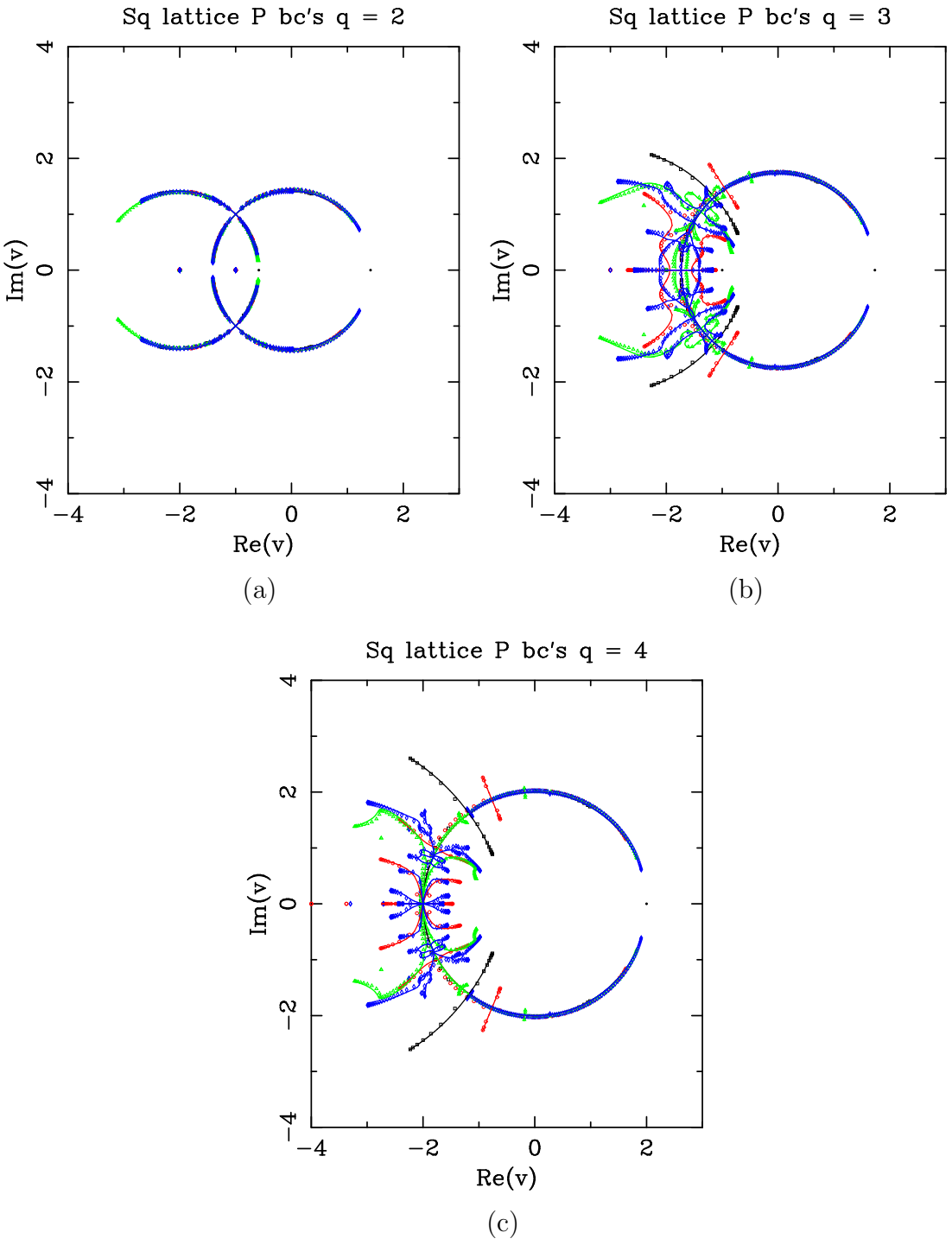


Figure 12: Limiting curves forming the singular locus $\mathcal{B}$, in the $v$ plane, for the free energy of the $q = 2$ (a) $q = 3$ (b), and $q = 4$ (c) Potts model on the $(L_t)_{\rm P} \times \infty_{\rm F}$ square-lattice strips with the following widths $L_t$: 2 (black), 3 (red), 4 (green), and 5 (blue). We also show the partition-function zeros for the strips $(L_t)_{\rm P} \times (10L_t)_{\rm F}$ for the same values of $L_t$. The color code is as in Figure 11.

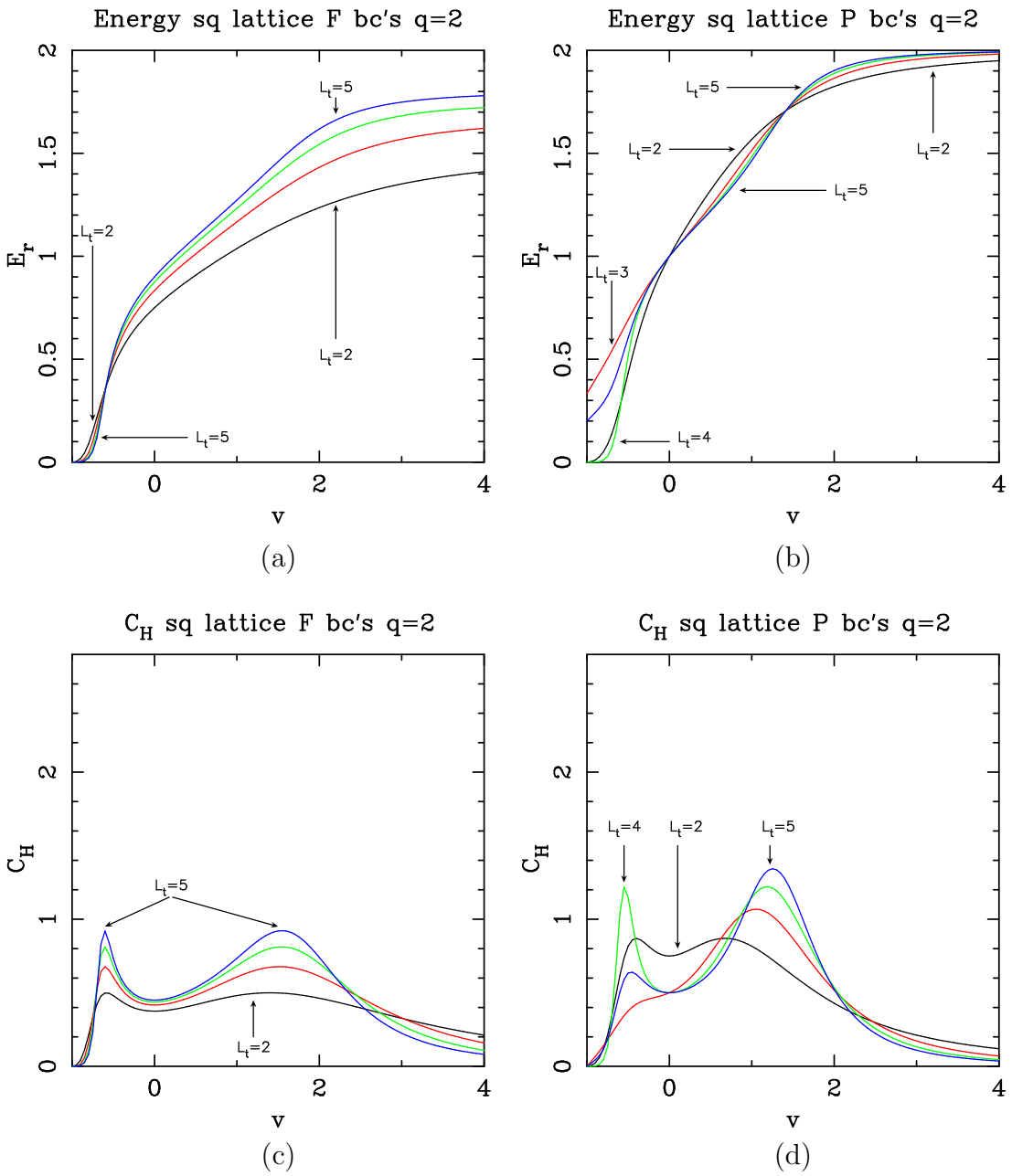


Figure 13: Reduced internal energy $E_r = -E/J$ and specific heat $C_H$ as functions of the temperature-like parameter $v$ for the $q = 2$ Potts model on square-lattice strips of size $(L_t)_{\rm F} \times \infty_{\rm F}$ and $(L_t)_{\rm P} \times \infty_{\rm F}$ with $2 \le L_t \le 5$. The plot includes both the ferromagnetic and antiferromagnetic Potts models, for which the temperature ranges are $0 \le v \le \infty$ and $-1 \le v \le 0$, respectively.

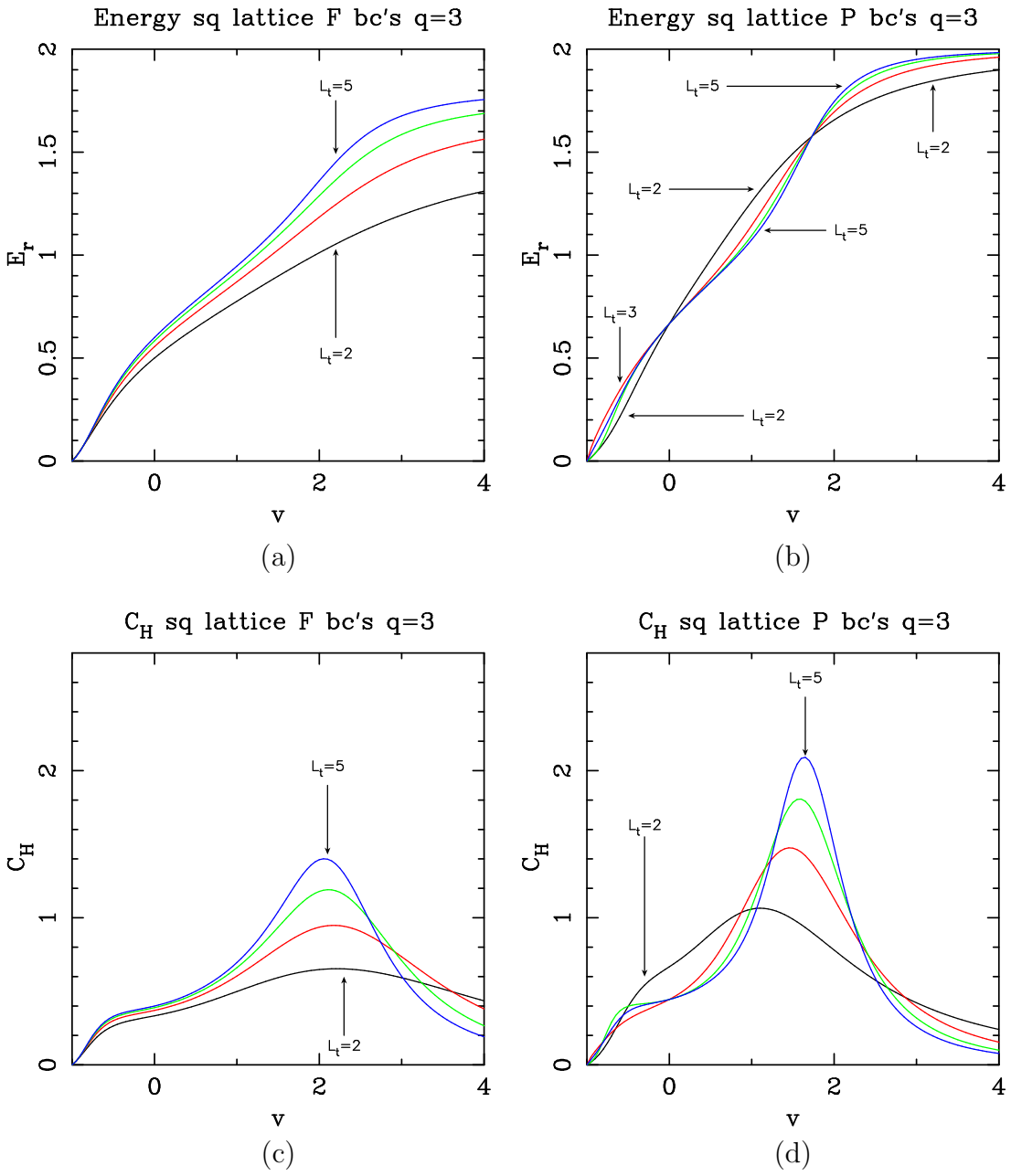


Figure 14: Reduced internal energy $E_r = -E/J$ and specific heat $C_H$ as functions of $v$ for the $q = 3$ Potts model on square-lattice strips of size $(L_t)_{\rm F} \times \infty_{\rm F}$ and $(L_t)_{\rm P} \times \infty_{\rm F}$ with $2 \le L_t \le 5$. Notation is as in Fig. 13.

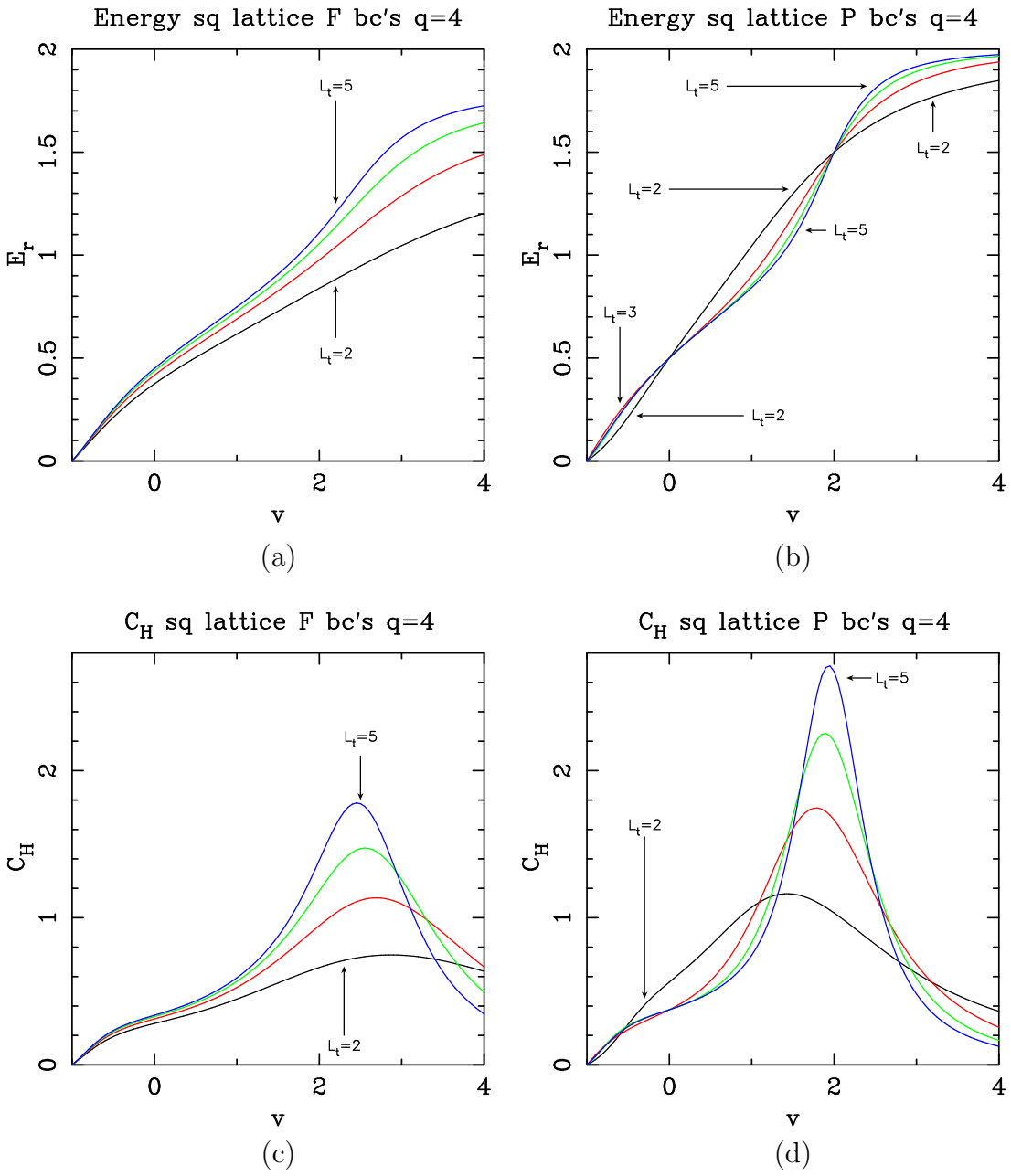


Figure 15: Reduced internal energy $E_r = -E/J$ and specific heat $C_H$ as functions of $v$ for the $q = 4$ Potts model on square-lattice strips of size $(L_t)_{\rm F} \times \infty_{\rm F}$ and $(L_t)_{\rm P} \times \infty_{\rm F}$ with $2 \le L_t \le 5$. Notation is as in Fig. 13.